

The “Missing Glaciations” of the Middle Pleistocene

Philip D. Hughes¹, Philip L. Gibbard², Jürgen Ehlers³

¹ Department of Geography, School of Environment, Education and Development,
The University of Manchester, Oxford Road, Manchester M13 9PL, United Kingdom

² Scott Polar Research Institute, University of Cambridge, Lensfield Road, Cambridge
CB2 1ER, United Kingdom

³ Hellberg 2a, D-21514 Witzeeze, Germany

Abstract

Global glaciations have varied in size and magnitude since the Early-Middle Pleistocene transition (~773 ka), despite the apparent regular and high-amplitude 100 kyr pacing of glacial-interglacial cycles recorded in marine isotopic records. The evidence on land indicates that patterns of glaciation varied dramatically between different glacial-interglacial cycles. For example, MIS (Marine Isotope Stages) 8, 10 and 14 are all noticeably absent from many terrestrial glacial records in North America and Europe. However, globally, the patterns are more complicated with major glaciations recorded in MIS 8 in Asia and in parts of the Southern Hemisphere, such as Patagonia for example. This spatial variability in glaciation between glacial-interglacial cycles is likely to be driven by ice volume changes in the West Antarctic Ice Sheet and associated interhemispheric connections through ocean-atmosphere circulatory changes. The weak global glacial imprint in some glacial-interglacial cycles is related to the pattern of global ice build-up. This is caused by feedback mechanisms within glacier systems themselves which partly result from long-term orbital changes driven by eccentricity.

1. Introduction

The most extensive and sustained glaciations in the Quaternary began in the last 900 kyr (*c.* MIS 24-22 to present) in the Northern Hemisphere and are associated with 100 kyr eccentricity-driven glacial-interglacial cycles (Head and Gibbard 2015; Hughes and Gibbard 2018). Despite the obliquity-driven shorter 41 kyr glacial-interglacial cycles of the earlier Pleistocene, there is evidence that high- and mid-latitudinal ice sheets in the North Atlantic region have been present since the beginning of the

Pleistocene (Thierens et al. 2012). Southern Hemispheric glaciation is an even longer-established phenomenon with substantial glaciation already a regular occurrence in the Tertiary (Ehlers et al. 2018).

In the Italian Dolomites, glaciation became established in MIS 22 (Muttoni et al. 2003). Comparable evidence is also found north of the Alps in Switzerland and southern Germany (Fiebig et al., 2011). However, the "Deckenschotter" glaciofluvial deposits in Switzerland may represent earlier glaciation, and the older "Höhere Deckenschotter" include vertebrate remains which suggest an age of 2.6-1.8 Ma (Bolliger et al. 1996). The "Höhere Deckenschotter" are regarded as glaciofluvial deposits. However, no till has been found as yet. In contrast, the "Tiefere Deckenschotter" contain tills. Glaciation then might have been more extensive than in the Würmian – see Figure 1 for global chronostratigraphical correlations. The age is uncertain, but the deposits clearly predate the Middle Pleistocene (Preusser et al. 2011) when Schlüchter (1989) identified a major phase of geomorphological change ("Mittelpleistozäne Wende") in the the Alps. The oldest glaciation identified in the Pyrenees is of late Cromerian age (MIS 16 or 14) (Calvet, 2004). In North America, widespread lowland glaciation (beyond Alaska and the Northern Territories) is first seen during MIS 22 or 20 (Barendregt and Duk-Rodkin, 2011; Duk-Rodkin and Barendregt, 2011). In South America, the extensive Great Patagonian Glaciation is dated to 1.1 Ma and correlated with MIS 30-34 (Singer et al. 2004).

Following the Early Pleistocene precursors, glaciers reached lowland northern Europe and Siberia in the early Middle Pleistocene shortly before the Brunhes–Matuyama palaeomagnetic reversal (773 ka), which represents the boundary between the Early and Middle Pleistocene (Head et al. 2008). These events laid down extensive sheets of glaciogenic deposits across wide areas both on land and beneath the sea. In the northern North Sea the formation of the Norwegian Channel caused an abrupt change of sedimentary conditions at about this time (Ottesen et al. 2014). Whilst 100 kyr cycles began c. MIS 24-22 (Elderfield et al. 2012), the largest amplitude 100 kyr glaciations started with MIS 16, which marked the completion of the Early-Middle-Pleistocene transition (Head and Gibbard 2005; Mudelsee and Schulz, 1997; Hughes and Gibbard 2018).

Subsequently, major ice sheets repeatedly extended over large regions of North America during the Middle Pleistocene pre-Illinoian events MIS 16, 12, 8 and 6 (Illinoian s.s.) and the Late Pleistocene MIS 4–2 (Wisconsinan). The Laurentide Ice Sheet formed over large areas of Canada, reaching as far south as 38°N in the United States during the Late Pleistocene (Dyke and Prest 1987) (Figure 2). More significantly, the change in ice volume between glacial-interglacial cycles was the largest single contribution to the global sea level changes. This was 70-90 m for the last glacial-interglacial cycle (Stokes et al. 2012), which represents well over half of the global ice contribution to glacial-interglacial sea level change. Today, the largest ice sheet is restricted to Greenland with much smaller ice caps present in Canada.

The marine oxygen isotope record provides the main basis for defining Quaternary glacial-interglacial cycles (Lisiecki and Raymo 2005) and has long been considered to represent a record of global ice volume (Shackleton 1967). The marine isotope record is widely used as the global reference with which the Quaternary can be subdivided and the scheme of stages and substages in marine isotope record continues to underpin the Quaternary timescale (Lisiecki and Raymo 2005; Railsback et al. 2015) (Figure 1). The marine isotope record has the advantage of being derived from quasi-continuous sedimentary sequences on the deep-ocean floors, whereas the glacier records on land are inherently fragmentary. However, the marine isotope record is a composite signal of fluctuations in global ice volume and does not provide information on the spatial pattern of glaciations. Furthermore, since changes in global ice volume are dominated by the Laurentide Ice Sheet (Figure 2) it is not necessarily representative of the pattern and scale of glaciations in other parts of the world. This poses problems for direct terrestrial-marine correlation (Gibbard and West 2000) and care must be taken to isolate glacier records using single proxies such as the marine isotope record. This is also true for other indirect proxies for global glaciations, some of which are utilized here such as sea level and ice core records. Thus, a collective approach is necessary to decipher the patterns of global glaciations, especially where terrestrial glacial records are absent, ambiguous or poorly dated, which is often the case especially for the Middle Pleistocene glaciations.

The application of numerical dating of Late Pleistocene glaciations is increasingly demonstrating the asynchronies in the timing of glacial maxima on a global scale (Hughes et al. 2013). Whilst the differing timing of mountain glaciations compared to the continental ice sheets has been known for decades (e.g. Gillespie and Molnar 1995), there is now also evidence that the timing of maximum extents of major ice sheet margins may have differed by as much as tens of thousands of years. Such differences appear to result from the contrasting regional geographical situation, where differing ocean and atmospheric circulatory patterns influence the precipitation and air temperatures (Hughes et al. 2013).

Differences in the pattern and timing of glacial extent are also notable between different glacial-interglacial cycles (cf. Margari et al. 2010; 2014; Hughes and Gibbard 2018; Batchelor et al. 2019). The largest glaciations of the last 800 kyr, such as in MIS 5d-2, were characterised by an early advance of glaciers followed by an interlude then a second major advance leading to the global glacial maxima within the glacial-interglacial cycles (Hughes and Gibbard 2018). This corresponds to the classic asymmetrical pattern of ice build-up in 100 kyr glacial-interglacial cycles (Broecker and van Donk 1970). The greater magnitude of the second major global ice advance is reflected in the larger dust peak associated with this compared to the first major advance, such as when comparing MIS 4 and 2 in the last glacial-interglacial cycle (Figure 3). However, Hughes and Gibbard (2018) identified differences between glacial-interglacial cycles with some exhibiting different patterns. For example, in MIS 10 and 8 the first phase of glacier build-up corresponded to the largest dust peaks and the later global glacial maxima was associated with much smaller dust peaks in Antarctic ice-core records (Figure 4). Other anomalies are also evident when considering the pattern of glaciations from the perspective of the marine isotope record. For example, some major stadials occur within interglacial complexes (such as MIS 7d) (Ruddiman and McIntyre 1982). These represent “missing glaciations” in the sense that they are rarely recorded on land. However, it is important to understand that glaciers would have been more extensive than today in most areas of the world in all cold intervals of major glacial-interglacial cycles. The evidence that glaciations are “missing” simply arises because their spatial coverage has been overridden by later more extensive glaciations.

We test the hypothesis that the cold phases of some glacial-interglacial cycles were characterised by less extensive glaciations than others. In order to do this, this article examines the evidence for Middle Pleistocene glaciations after MIS 16, which marked the onset of the largest 100 ka glacial cycles (Hughes and Gibbard 2018). We focus on MIS 8, 10 and 14 together with other intermediate intervals (MIS 7d, MIS 13b and 15b) and test whether the concept of “missing glaciations” is valid for these cold intervals. We aim to explore reasons for the differences in the terrestrial glacial records between and within glacial-interglacial cycles by examining both the wider environmental imprint of global glaciations alongside the drivers of global climate change.

2. Methodological Approach

2.1. Glacial records

The geological and geomorphological evidence for glaciation is based on numerous published papers from sites around the world. This evidence includes large compilations and reviews such as those in Ehlers et al. (2011a, b) and many other sources, including many new datasets from the last few years. A key focus is on dated records, which for the Middle Pleistocene glacial record are dominated by cosmogenic exposure, optically stimulated luminescence, and uranium-series dating.

2.2. Indirect records of glaciation and global climate

2.2.1. Marine isotope records

Marine oxygen isotope records provide the classic proxy for global ice volume (Shackleton 1967) and underpin modelling approaches for ice sheet reconstructions through time where direct evidence of glaciation is not available (e.g. Batchelor et al. 2019). The driver of cyclic fluctuations in marine oxygen isotopes from foraminiferan tests has long been attributed to orbital forcing (Hays et al. 1976) and this provides the timeframe to which the marine isotope record is tuned (Imbrie et al. 1984, Ruddiman et al. 1989; Lisiecki and Raymo 2005) (Figure 4). However, the marine oxygen isotope record is not a pure record of global ice volume but is a record of both global ice volume and deep ocean temperature (Spratt and Lisiecki 2016).

Furthermore, as noted earlier, changes in the Laurentide Ice Sheet through glacial-interglacial cycles dominate the global ice volume component of the marine isotopic signal due to its large size relative to other ice masses on Earth (Figure 2). Consequently, the marine isotope record is not representative of the spatial complexity of global glaciations (Hughes et al. 2013).

2.2.2. Sea-level records

Global ice volume is closely intertwined with global sea levels and the magnitude of glaciations is reflected in sea-level changes. Global sea levels through the last 800 kyr were assessed using the data of Spratt & Lisiecki (2016) (Figure 4). In their paper, Spratt and Lisiecki (2016) analysed seven Late Pleistocene sea-level records for the interval 0-430 kyr and five for the interval 0-798 kyr that have converted the oxygen isotope content of the calcite tests of foraminifera ($\delta^{18}\text{O}_c$) to sea level. The seven records included an inverse ice volume model (Bintanja et al., 2005), Pacific benthic $\delta^{18}\text{O}$ of seawater ($\delta^{18}\text{O}_{sw}$) (Elderfield et al., 2012), a global stack of planktonic $\delta^{18}\text{O}_{sw}$ (Shakun et al., 2015), Relative Sea Level from the Mediterranean (Rohling et al., 2014), Atlantic benthic $\delta^{18}\text{O}_{sw}$ (Sosdian and Rosenthal, 2009), $\delta^{18}\text{O}_c$ regression (Waelbroeck et al., 2002) and a Relative Sea Level from the Red Sea (Rohling et al., 2009). The longer record (used in this paper) for interval 0-798 kyr excluded the $\delta^{18}\text{O}_c$ regression (Waelbroeck et al., 2002) and the Relative Sea Level from the Red Sea (Rohling et al., 2009) (see Spratt and Lisiecki 2016, their Table 1).

Hughes and Gibbard (2018) analysed sea-level changes through glacial-interglacial cycles using the data of Shakun et al. (2015), who used planktonic $\delta^{18}\text{O}_{sw}$ to correct the $\delta^{18}\text{O}$ stack for non-ice volume effects. However, in their analysis of global sea-level change through glacial-interglacial cycles, Spratt and Lisiecki (2016) noted that because the surface ocean is affected by greater hydrological variability and characterises a smaller ocean volume than the deep ocean, then planktonic $\delta^{18}\text{O}_{sw}$ may differ more from ice volume changes than benthic data.

2.2.3. Sea-surface temperature records

Shakun et al. (2015) exploited the temperature component of planktonic $\delta^{18}\text{O}$ records from 49 cores around the globe to calculate a stacked record of global sea surface temperatures (Figure 4). This now enables insights into global shifts in both climate

and ice volume during glacial-interglacial cycles. This is significant because it avoids the Laurentide problem, where global ice volumes are dominated by a single regional ice mass. Whilst ice sheets do affect sea-surface temperatures at the regional scale, global sea-surface temperatures between different oceans are much less likely to be dominated by regional ice dynamics.

Whilst the surface ocean is undoubtedly subject to greater hydrological variability (cf. Spratt and Lisiecki 2015) and surface atmospheric processes, this is useful for gauging the state of the Earth's ocean-atmosphere interface. At individual scales, sea-surface temperature records are likely to be quite variable, but when combined the stack of 49 cores utilized by Shakun et al. (2015) from sites located at 0-60 N and S in the Pacific, Atlantic and Indian Oceans does provide a global summary of the state of the ocean-atmosphere interface through glacial-interglacial cycles.

2.2.4. Ice-core records

Dust content in polar ice cores can provide insights into the state of the global atmosphere through time and this was utilized by Lambert et al. (2008; 2012) to assess dust flux over Antarctica during multiple glacial-interglacial cycles. Hughes and Gibbard (2018) argued that peaks in Antarctic dust in glacial-interglacial cycles corresponded to global ice build-up in both hemispheres and this was used as an indirect indicator of global glacial behaviour in glacial-interglacial cycles. This argument was largely built on the observations from the last glacial-interglacial cycle where large ice build-up in MIS 4 and 2, for example, was associated with peaks in dust not only in Greenland but also in Antarctica (Hughes et al. 2013) (Figure 3).

Given that the Greenland ice-core records only span from the last Interglacial, Antarctic records must be relied upon for earlier glacial-interglacial cycles. Dust flux over Antarctica has a close correlation with temperature as climate becomes colder (Lambert et al. 2008). Comparison of Antarctic ice-core dust records with loess/palaeosol sequences from the Chinese Loess Plateau (Kukla et al. 1994) confirms the synchronicity of global changes in atmospheric dust load (Lambert et al. 2008). However, being a Southern Hemisphere record, comparisons of dust peak magnitudes cannot necessarily be transferred to interpreting the size of global ice volume, only the temporal pattern and possibly the hemispheric distribution of ice

masses. Nevertheless, Antarctic dust records are broadly representative of the global hydrological cycle with increasing dust indicating a cooler and drier global atmosphere that is directly associated with the extent of global glaciations.

Dust records may be a better reflection of global ice spatial coverage on land than marine isotope records, which partially reflect ice volume. This is because increased ice coverage over land surfaces causes increased aridity in peripheral areas due to the effects of ice masses on regional climate (Manabe and Broccoli 1985). This occurs today where strong anticyclones form over modern ice sheets (Hobbs 1945). The aridity effects would have been compounded during the Pleistocene cold phases due to effects of not just low precipitation but also low atmospheric CO₂ on plant growth (Claquin et al. 2003).

2.3. Drivers of global glaciations - Solar forcing and CO₂

We examine the patterns of Earth-orbital changes and glacial-interglacial cycles to see if there is any relationship between “missing glaciations” and orbital forcing. Solar radiation is important when considering glaciations because it controls the energy receipt to the Earth and thereby impacts on glacier mass balance, especially ablation. In their synthesis of the last ten glacial-interglacial cycles, Hughes and Gibbard (2018) showed that variations in solar radiation in the Northern Hemisphere was responsible for ~50-60% of variations in global ice volume. For example, troughs in solar radiation at the end of interglacials and beginning of subsequent cold stages are thought to be associated with rapid glacier advances in the continental interiors and high- and mid-latitude mountains (Hughes and Gibbard 2018). This hypothesis is tested further here by quantifying the magnitude of solar peak-trough changes at the transition between interglacial and glacial intervals (Figure 4). This was done by calculating a value for **solar-trough magnitude (STM)**, which describes the trough magnitude and timespan at 60°N. This is derived by taking the median (50th percentile) solar radiation value (W m⁻²) between the trough and the preceding peak (s_m) and dividing this by the trough timespan (s_t) (defined by the time in years between the trough and the preceding peak), then inverting this value:

$$STM = 1/(s_m/s_t)$$

We also examine the orbital record further by isolating the effects of orbital parameters such as eccentricity, obliquity and precession, on global glacier dynamics within and between glacial-interglacial cycles. Eccentricity controls the shape of the Earth's orbit around the sun and directly affects the influence of variations of precession (i.e. on the timing of peri- and aphelion), and the seasonal distribution of solar radiation. The interaction of eccentricity with precession is indicated in the precession index (Figure 4). In addition to solar radiation, Ganopolski et al. (2016) highlighted the importance of CO₂ in glacial inception. They identified points in time where low CO₂ corresponded with low insolation as potential triggers for global ice build-up. This hypothesis implies that low insolation alone cannot explain global glacial inception. Instead, it is the combination of insolation forcing with atmospheric CO₂ concentrations that drives glacial inceptions. Over the longer term, declining atmospheric CO₂ through the Quaternary has been linked to the removal of weathered regolith by glacial erosion over North America and Europe (Clark and Pollard 1998). This causal mechanism may partly explain the transition to the large-magnitude 100 ka glacial-interglacial cycles at the Early-Middle-Pleistocene transition (Clark and Pollard 1998; Ganopolski and Calov 2011; Tabor and Poulson 2016; Willeit et al. 2019).

2.4 Terminology

There are three ways to define glacial-interglacial cycles (Hughes and Gibbard 2018):

- 1) The periods between glacial terminations.
- 2) The periods of cold phases defined by global sea surface temperatures within glacial-interglacial cycles (cf. Shakun et al. 2015), and;
- 3) The span of traditional subdivision of cold intervals based on Marine Isotope Stages and substages (Railsback et al. 2015).

The term “cold stage” refers to climatostratigraphical/chronostratigraphical units such as the Weichselian or Wisconsinan in Europe or North America, respectively, which are equivalent to MIS 5d-2. This is complicated by the fact that some cold stages in this definition span multiple glacial-interglacial cycles, such as the Saalian and Wolstonian Stages in continental Europe and the British Isles, respectively. Marine oxygen isotope stages are distinct from chronostratigraphical cold stages and

sometimes multiple Marine Isotope Stages make up a single cold stage in the strict sense. For example, the Weichselian/Wisconsinan stages include MIS 5d-2 and also the early part of MIS 1. A global correlation table based on the chart of Cohen and Gibbard (2011) is provided in Figure 1 to aid cross-comparison between marine isotope events and terrestrial chronostratigraphy.

3. The “missing glaciations”

3.1. MIS 8 (Middle Saalian and equivalents)

MIS 8 occurs within a larger glacial-interglacial cycle between termination IV and III (Figure 4). Overall, this was a relatively weak glacial-interglacial cycle. The glacial inception occurred at the boundary of MIS 9d/e at c. 320 ka. MIS 8 has a weak signal of global glaciation in many records, particularly benthic $\delta^{18}\text{O}$ (Lang and Wolff 2011) and second only to MIS 14 in terms of maximum $\delta^{18}\text{O}$ values for the last ten glacial-interglacial cycles (Figure 4). At -93.27 m, MIS 8 had the highest sea levels of the last six 100 kyr glaciations (Table 1). The lowest sea levels do not coincide with the trough in benthic $\delta^{18}\text{O}$ values (at 252 ka) but occurred c. 18 kyr earlier at 270 ka in MIS 8c (Figure 4). A strong interstadial (MIS 9a) separates two marine isotopic troughs (MIS 8a-c and 9b).

The solar-trough magnitude at the beginning of this glacial-interglacial cycle was one of the weakest of the seven glacial-interglacial cycles (Table 2). This is likely to have resulted in a weak glacial inception and explains the weak stadial conditions in MIS 9d, which is characterised by relatively minor excursions in benthic and planktonic isotope values and moderate influence of sub-polar water masses (Roucoux et al. 2006). In their core from the Iberian margin, Roucoux et al. (2006) argued that the pollen evidence suggests a less arid and cold climate than during other stadial intervals where steppe was more abundant, and temperatures offshore were lower.

Dust flux over Antarctica for MIS 8 reached some of the highest and sustained levels of the last million years, reaching values comparable with MIS 6, yet more sustained, and greater than MIS 5d-2 (Figure 4). Significantly, the dust peak in Antarctica does not coincide with the largest marine isotope trough of MIS 8a. Instead, it occurs earlier at c. 272 ka in MIS 8c, coinciding with the lowest sea levels. Hughes and

Gibbard (2018) noted that the first dust peak also coincides with the lowest CO₂ levels (Ganopolski et al. 2016) and the coldest global sea surface temperatures of this glacial period (Shakun et al. 2015). Pollen records from a marine core on the Iberian margin match these patterns and show the most extreme glacial conditions of MIS 8 occurred during the early part, followed by an interval of warmer conditions and tree population expansion after 263 ka (Roucoux et al. 2006). This suggests that the configuration of controls of global climate (including insolation, atmospheric composition, land cover, sea ice and the ice sheets themselves) were different in MIS 8 from other glaciations, such as MIS 6 and 5d-2. In these later glaciations, the global ice maxima and associated cold and dry indicators occurred towards the end of the glacial-interglacial cycle.

Examination of the record of glaciation during this period (i.e. c. 300-245 ka) repeatedly shows that evidence of glaciation is poorly represented throughout much of the world's glaciated regions. In northern Europe the traces of glaciation that can be reliably attributed to this time are rare. The few deposits that have been identified in North-West Europe are mainly based on isolated numerical age determinations, especially optically stimulated luminescence (OSL) or amino-acid racemisation analyses of adjacent sediments or their contained fossil materials. For example, the most often quoted example is that reported by Beets et al. (2005) suggesting that pre-Late Saalian (i.e. Middle Saalian; MIS 8) till occurs in the North Sea basin based on geophysical, micropalaeontological and amino-acid age evidence. Whilst there is no question that till occurs at the site, there remains scepticism about the age attribution among Dutch workers who generally attribute these deposits to the Late Saalian (MIS 6; Cohen 2017, personal communication). Despite other possible MIS 8 records from other circum-North Sea localities (e.g. Davies et al. 2012; White et al. 2010; 2017; Bridgland et al. 2014; Roskosch et al. 2015) all of these remain equally equivocal. In contrast, as in the Netherlands, recent dating evidence from eastern England has confirmed that a major glaciation did occur in MIS 6 (Evans et al. 2019) confirming the Wolstonian (=Saalian) age of a glaciation that reached into the Fenland basin in eastern England (Gibbard et al. 2018). The lack of a regional till sheet and consistent biostratigraphy appears to support the view that glacial ice did not extend into the central western European area and the central and southern North Sea basin (Huuse 2017, personal communication) during MIS 8. However, there is evidence for Middle

Saalian glaciation that reached the continental shelf edge off-Norway, Svalbard and Scotland, according to Sejrup et al. (2000; 2005). In southern Jæren this glaciation is represented by the Vigrestad Till (glacial F: Sejrup et al. 2000). In Denmark westward flowing meltwater streams deposited sand and gravels over much of central and southern Jylland. These streams derive from the first Saalian ice advance that occurred during MIS 8, which deposited the Treldenæs Till (Houmark-Nielsen, 2004, 2011). This Norwegian Saale Advance invaded Denmark from the north, probably terminating south of the Danish-German border in Schleswig-Holstein (Houmark-Nielsen 2011).

In North-West Europe, Toucanne et al. (2009a) noted that ‘Fleuve Manche’ fluvial discharge through the English Channel was significantly less during MIS 8 than during MIS 6 and MIS 2 (indicated by lower mass accumulation rates (MAR) in Figure 6). This is consistent with smaller ice masses in northern Europe and the Alps, the meltwater from which drained into this river system in MIS 8. Furthermore, in the Northeast Atlantic Ocean at ODP 980 (55°29’N, 14°42’W) summer sea-surface temperatures were generally warmer in MIS 8 than in MIS 6 and 2 (McManus et al. 1999). However, oscillations in SSTs were large with minimum temperatures on a par with MIS 6 and 2. In fact, the quantities of ice rafted debris in the NE Atlantic during MIS 8 and 10 were significantly larger than in MIS 6 and 2 (McManus et al. 1999). This was related to high-amplitude millennial scale climate change, which is also reflected in terrestrial vegetation records in Europe (Fletcher et al. 2013). The muted signal in the ‘Fleuve Manche’ discharge in contrast to a strong signal in the ice-rafted debris (IRD) in the NE Atlantic suggests the configuration of ice masses in this region differed between glacial-interglacial cycles.

In Poland, the Krznanian glaciations are correlated with MIS 8 (Lindner and Marks 1999). According to Marks (2011) Poland was invaded by ice sheets derived from Scandinavia during the Liwiecian, Krznanian and Odranian intervals within the Saalian Stage. The limit of the Odranian glaciation can be mapped at the modern land surface, whereas the Liwiecian and Krznanian are buried by younger deposits. During the latter an ice sheet advanced into eastern Poland, reaching as far south as the northern foreland of the South Polish Uplands, and it probably also approached

the Silesian Upland. This advance may have also crossed the Baltic States, Latvia and Lithuania and presumably parts of Belarus.

In neighbouring European Russia, glaciation during this period seems to have been markedly less extensive than during the Late Saalian-equivalent Dniepr and Moscow glaciations (MIS 6) (Velichko et al. 2011) (Figure 1). However, east of the Urals it is represented by the substantial till of the Samarovo glaciation, the deposits of which form the maximum glacial drift boundary in western Siberia. This major glaciation is correlated with MIS 8 (Figure 5) based on regional stratigraphical successions (Astakhov et al. 2016).

Whilst the limit is based on boreholes and rare natural sections in the West Siberian Plain, in the Central Siberian uplands the boundary has been mapped based on chains of push moraines and occasionally where it overlies interglacial fluvial deposits in buried valleys (Rudenko et al., 1984; Astakhov 2011). In the Western Siberian Plain and the Central Siberian Plateau the Samarovo glaciation was consistently much more extensive than the later Taz glaciation which is thought to date from later in the Saalian Stage in MIS 6 (Astakhov et al 2016). Given the scale of the land areas involved these Siberian ice masses would have been major contributors to global ice volume.

In the mountains of central and southern Europe, evidence of glaciation in MIS 8 has been recognised in Iberia (Fernández Mosquera et al. 2000; Vidal Romaní *et al.* 2015), Italy (Giraudi and Giaccio 2017) and in the Alps (Preusser et al. 2011). In Baden-Württemberg and Bavaria the multi-phased Riss Glaciation is provisionally correlated with MIS 10-6 (Doppler et al. 2011). In the Balkans there is also some evidence of MIS 8 glaciation (Hughes et al. 2011). In the Italian Apennines, Giraudi et al. (2011) reported that there was no evidence for glaciation in MIS 8, unlike for other Middle Pleistocene glaciations. However, later work in the same basin revealed evidence of two glaciations between 350 and 130 kyr and these were correlated with MIS 8 and 6, although the relative sizes of these two glaciations was not established (Giraudi and Giaccio 2017).

In North America evidence of glaciation attributed to the MIS 8 interval is equally elusive. In North-West Canada and eastern Alaska where till and associated deposits of the Reid Glaciation are frequent (Duk-Rodkin et al. 2004; Duk-Rodkin and Barendregt 2011), there is some doubt regarding the correlation of these materials to either MIS 6 or 8, both, or in some cases younger intervals (Ward et al., 2008; cf. Duk-Rodkin et al. 2004; Barendregt & Duk-Rodkin 2011 for discussion). In some areas, OSL dating of glaciofluvial deposits over- and underlying till has determined the age of the Reid Glaciation as MIS 6 (Demuro et al. 2012). Equivalents to the MIS 6 or 8 glaciations are almost certainly present in the Mackenzie Mountains, where as many as three tills occur beneath the Late Pleistocene Laurentide glacial deposits at the surface. On Banks Island in the Canadian Arctic, till underlying last interglacial (Sangamonian Stage) Cape Collinson glaciomarine deposits are termed the Thomsen Glaciation (250 ka). These deposits are thought to mark the maximum extent of Middle Pleistocene glaciation in north-western Canada (Duk-Rodkin et al. 2004).

Elsewhere in North America evidence is found in the Sierra Nevada where several till units appear to date from the MIS 8–6 (303–186 ka) interval, but here the age control is insufficient to distinguish to which individual events they relate (Gillespie & Zehfuss 2004; Gillespie and Clark 2011). Despite previous reports of MIS 8-age glacial deposits in Glacier National Park, the early Bull Lake Till (Richmond 1986), it is now thought that no deposits of this age occur in this district (Fullerton et al. 2004). In Illinois, the southern margin of the Middle Pleistocene Laurentide Ice Sheet extended 150 km beyond the later Wisconsinan (MIS 5d–2) limits. Stiff & Hansel (2004) suggested that glacial deposits of MIS 8 may be present in these more extensive limits. However, Curry et al. (2011) argue that the combination of evidence from palaeosols and a range of different dating techniques (OSL, ^{10}Be , amino-acid geochronology) indicate that the Illinoian glaciation is restricted to MIS 6. In Missouri, till units have been shown to pre-date MIS 6 using ^{10}Be burial dating, although the imprecision of this technique means that correlations for these tills can be made with MIS 8, 10 or even 12 (Rovey and Balco 2011). In western Wisconsin two till formations are related to the ‘Illinoian Glaciation’ (*s.l.*) which in the region is dated to 300–130 ka (Syverson & Colgan 2004, 2011). These units, derived from the Superior province, extend beyond the Wisconsinan ice-maximum limits. However it is not known to which marine isotope stage they relate. Patchy deposits of similar age

occur in southern Wisconsin and northern Illinois (Syverson and Colgan 2004; 2011), but again may relate to MIS 6.

In South America evidence from the tropics is once again rather limited, although there is strong evidence of MIS 8 glaciation in Patagonia. Here, ^{10}Be concentrations in outwash cobbles indicate a major glacial advance at c. 260 ka, within MIS 8. This is coincident with the most pronounced dust peak in MIS 8 in Antarctic ice cores (Hein et al. 2009). Significantly, Hein et al. (2009; 2017) found that exposure ages from dated outwash terraces are 70-100 ka older than the associated moraines. Based on geomorphological observations, they suggested that this difference can be explained by exhumation of moraine boulders.

Elsewhere in the Southern Hemisphere, the large moraines occurring at the mouths of valleys and cirque basins in western Tasmania were thought to have marked the Last Glaciation (MIS 2) limits, such as in the West Coast Range (Lewis, 1945; Colhoun, 1985). However, recent exposure dating has demonstrated that this is incorrect and that some of these moraines were formed during the Middle Pleistocene (Barrows et al., 2002; Kiernan et al. 2010). In their review, Colhoun & Barrows (2011, p. 1042) stated that the Hamilton Moraine, west of Lake Margaret, formed during MIS 8.

In New Zealand, weathered till, correlated with MIS 8 (Rattenbury et al., 2006), near Edwards Pass between the Waiau and Clarence valleys, lies about 20 km down valley from the MIS 2 termini. However, a geochronological basis for this correlation is lacking and for most glaciations pre-dating MIS 6 correlations with the marine isotope record are made using relative and biostratigraphical criteria (Barrell 2011). With respect to the Middle Pleistocene glaciations in New Zealand, only MIS 6 glaciations have been confirmed by dating (e.g. Rother et al. 2010).

Overall, glaciation associated with MIS 8 is rarely found or at least not conclusively confirmed in most regions. Glacier extents in MIS 6 were consistently larger and this is supported by a much wider body of evidence. Major exceptions to this occur in Russia east of the Urals and in Patagonia.

3.2. MIS 10

Superficially, the isotope sequence for MIS 10 resembles those of other major glaciations, with a similar structure to MIS 12, but less severe. For example, global sea-levels were -102.83 m compared with -124.4 for MIS 12, yet >9 m lower than in MIS 8 (Table 1). However, the dust record from Antarctica indicates two major dust peaks, one at c. 341-342 ka corresponding with the ‘glacial maximum’ indicated in the marine isotope record (MIS 10a) and another even larger dust peak earlier in the glacial-interglacial cycle at c. 355 ka (Figure 4). The largest dust peak occurs in substage MIS 10b and corresponds with an early sea level trough of -92.82 at 356 ka. This dust peak and low sea level stand is preceded by the coldest part of MIS 10 (at the start of MIS 10c) recorded in global sea-surface temperatures (Figure 4; Shakun et al. 2015) and the lowest atmospheric CO₂ levels of the glacial-interglacial cycle (Hughes and Gibbard 2018).

Solar radiation in the Northern Hemisphere was lowest late in the glacial-interglacial cycle, close in time to the glacial maximum indicated in the marine isotopic record (Figure 4). Before this insolation was relatively high and sustained at >480 W m⁻² with only minor troughs earlier in the glacial-interglacial cycle, except for a more significant trough at the MIS 11c/11b boundary which marks the beginning of the glacial-interglacial cycle. The solar-trough magnitude at the preceding interglacial/glacial transition was weakest of all the last seven glacial-interglacial cycles (Table 2).

Like MIS 8, glacial deposits dating from the interval represented by MIS 10 (c. 375-340 ka) are very poorly represented in North-West Europe. In the southern and central North Sea region there is no record, although Norwegian and Svalbard ice extended to the shelf-margin as indicated in offshore accumulations, according to Sejrup et al. (2005) and is confirmed by IRD. The glaciation is represented by an unnamed till, underlying the Varhaug marine sediments in the Hobberstad borehole (Sejrup et al. 2000). In North Sea surveys Graham (2007) mapped ice-stream bed structures within the Coal Pit Formation, in the Witch Ground basin. Although the age correlation in this basin is not ideal, the features suggest shelf glaciation between MIS 10–6 (Graham et al. 2011). However, as in MIS 8 the ice was most probably markedly more limited in extent. Scandinavian and British ice masses were almost certainly not confluent across the North Sea basin during these phases (Toucanne et al., 2009a, b).

As with the MIS 8 evidence, there are some isolated age determinations that did hint at possible MIS 10-age glacial advances, e.g. Scourse et al. (1999) in the Nar Valley area of Norfolk in eastern England. However, these determinations have been questioned and more recently rejected (Gibbard & Clark 2011). Whilst ice masses over NW Europe were restricted in MIS 10, there was nevertheless significant ice-rafting in the North Atlantic reaching as far south as the Bay of Biscay (e.g. McManus et al. 1999; Toucanne et al. 2009a) (Figure 6).

Elsewhere in Europe the evidence for MIS 10-equivalent age glaciation is fragmentary. In the Alps, glaciation may have happened, but the evidence has not been dated (Van Husen & Reitner, 2011). Poland once again preserves a record of post-Holsteinian (Mazovian) Interglacial Stage glaciation that has been correlated with MIS 10. This Liviecian glaciation was the first glacial episode of the Saalian Stage (s.s.) and preceded the Zbójnian Interglacial. During this event, the ice sheet reached central Poland (Lindner and Marks 1999).

In Russia glacial deposits that have been reliably attributed to MIS 10 are very rare. However, Astakhov (2004; 2011) suggested that a sequence found in Siberia possibly represents a transition between Marine Isotope Stages (MIS) 10–9 where deep-marine sedimentation resulting from isostatic loading from the previous phase of glaciation is found. This dating is based on electron spin resonance (ESR) and green stimulated luminescence (GSL) ages of 300–400 ka. Similar ages have been reported for marine deposits from a few localities on the Taymyr Peninsula (Bolshiyarov et al., 1998). If this interpretation is correct, then it implies the development of a substantial ice cap over northern Siberia in MIS 10.

In North America, there is evidence of glacial advances into Pennsylvania during the Middle Pleistocene (pre-Illinoian A or B—MIS 10 or 12; i.e. Early Saalian and Elsterian) and overlain by late Middle Pleistocene (MIS 6—Illinoian or Late Saalian) (using the terminology of Richmond and Fullerton, 1986) deposits (Braun, 2011). Deposits possibly relating to MIS 10 may be present in the Stikine Valley in north-western British Columbia where they underlie basalt dated by K-Ar to 300±30 ka (Spooner et al. 1996; Duk-Rodkin and Barendregt 2011).

In the southern hemisphere there is little evidence in the glacier record of MIS 10 glaciation. However, in the Western Arthur Range of southwestern Tasmania cosmogenic exposure dating suggests that moraines were formed by glaciations in MIS 6 and 10 but not in MIS 8 (Kiernan et al. 2010). However, Kiernan et al. (2010) do acknowledge that the MIS 10 age may be an over-estimate if the erosion rates are too high, and in that case the moraines would be MIS 8 in age.

3.3. MIS 14

MIS 14 was characterised by limited global ice extent. The signal of climatic/environmental change is particularly weak in a range of records, marine and terrestrial, leading Lang and Wolff (2011, p. 375) to argue that “it is sufficiently weak that one could question its designation as a glacial”. In the marine isotope record the maximum $\delta^{18}\text{O}$ value of this cold stage was 4.55 at 548 and 536 ka, which is the lowest $\delta^{18}\text{O}$ value of all the last ten cold stages (Figure 4). Ice volume was the lowest of all the last ten glacial-interglacial cycles with global sea levels much higher than in other cold stages at -67.39 m at 537 ka (Table 1; Figure 4). Sea levels reached -62.75 m at 550 ka and remained depressed through to MIS 13b (-55.45 m), suggesting that the definition of this glaciation spans a longer interval than just MIS 14, despite termination IV being recorded in the marine isotope record and a sharp rise in global sea-surface temperatures at this time (Figure 4). The start of MIS 14 was associated with the strongest solar-trough magnitude of the last seven glacial-interglacial cycles (Table 2). However, this was mitigated by the fact that preceding peak in solar radiation (and median peak-trough value) was the largest solar peak at the glacial inception of the last seven glacial-interglacial cycles. Despite the evidence of limited global ice extent, global sea surface temperatures during MIS 14 were as cold as other cold stages that were characterised by much bigger glaciations (Shakun et al. 2015). The Antarctic dust signal for MIS 14 is much weaker than for any other glacial-interglacial cycles with dust flux $< 12 \text{ mg/m}^2/\text{a}$. A double peak pattern is evident at c. 540 and 530 ka with the first peak larger than the second (Figure 4).

There is little direct evidence of glaciation on land from MIS 14, probably because it was limited in extent compared to later glaciations. However, in the Italian Apennines a glacier advance has been dated to MIS 14 by applying $^{36}\text{Ar}/^{40}\text{Ar}$

dating to tephra deposits in a pro-glacial lacustrine sequence in the Campo Felice basin (Giraudi et al. 2011).

3.4. The glaciations that didn't make it: MIS 7d, MIS 13b and 15b

Some intervals characterised by major excursions in the marine oxygen isotope curve do not fit the criteria for definition as glacial-interglacial cycles as set out in Hughes and Gibbard (2018). Furthermore, they often do not conform to the conventional “sawtooth” model of 100 ka glacial cycles, such as MIS 7d (Ruddiman and McIntyre 1982). They either do not end in formally defined terminations, are insufficiently cold as recorded in proxies such as global SSTs, or have not been assigned full stage status in the marine isotopic record. In Antarctic dust records from MIS 7d, 13b and 15b the dust flux is relatively insignificant compared with full glacial-interglacial cycles. Whilst Antarctic dust flux cannot be directly related to global ice volumes only patterns of change, it nevertheless suggests that these intervals did not have significant effects on the global hydrological cycle. However, MIS 7d, 13b and 15b are each represented by high amplitude excursions of the $\delta^{18}\text{O}$ curve in the marine isotope record and their magnitude stands out compared with other stadials within glacial-interglacial cycles (Figure 4).

MIS 7d is the most pronounced of the three anomalous isotopic stadials (cf. Ruddiman and McIntyre 1982) and had a $\delta^{18}\text{O}$ value almost as high as MIS 14 in the stacked record of Lisiecki and Raymo (2006). In fact, in the sea-level stack of Spratt and Lisiecki (2016) MIS 7d has a slightly lower sea level than MIS 14, at -68.74 m (MIS 7d) versus -67.39 m (MIS 14) (Table 1; Figure 4). In other indicators such as Shakun et al.'s (2015) global sea-surface temperature stack, MIS 7d is a significant stadial but MIS 14 is much colder. In the same record both MIS 13b and 15b are insignificant events yet they recorded global sea levels at -55.45 and -54.4 m, respectively, and with large isotopic excursions in the marine $\delta^{18}\text{O}$ record (Figure 4). This suggests that these glaciations represented large regional but not global glaciation events. The very weak dust signal in the Antarctic ice core record also suggests that these glaciation events were confined to the Northern Hemisphere (Figure 4). In the Northern Hemisphere, very low arboreal pollen percentages in southern Europe indicate that MIS 7d was associated with very dry and cold conditions (Roucoux et al. 2008). This is associated with a major trough in Northern

Hemisphere summer radiation, the lowest of the past 800 kyr. The brevity of the stadial is likely to be explained by the subsequent peak in solar radiation in the Northern Hemisphere, which was the highest of the past 800 kyr (Figure 4).

The problem of defining glacial-interglacial cycles using the marine isotopic record is further compounded by the recognition or non-recognition of terminations. Technically, MIS 7d could be classified as part of a glacial-interglacial cycle based on terminations because it is bounded by terminations III (243 ka) (McManus et al. 1999; Lisiecki and Raymo 2006) and IIIa (225 ka) (Cheng et al. 2009). The age of IIIa at 225 ka, derived from U-series dating of a Chinese speleothem (Cheng et al. 2009), differs from the marine isotope curve, which shows a typical sharp transition slightly later at c. 219-220 ka. This may be an artefact of the age model used in the Lisiecki and Raymo (2005) LR04 stack. In fact, Cheng et al. (2009) found that variations in other marine isotopic records such as that at ODP 980 (McManus et al. 1999) were 3 kyr too young when compared with high resolution dated speleothem records.

MIS 7d represents an anomaly for the preceding and succeeding glacial-interglacial cycles of MIS 9a-8 and MIS 6 because Hughes and Gibbard (2018) defined these cycles as spanning terminations IV-III and IIIa-II, respectively. In this sense MIS 7d and the interval between terminations III and IIIa represent a truly “missing” glaciation if defined using terminations as the bounding criteria. The main characteristic that defines MIS 7d as a stadial, rather than a full glacial, is its length, which between terminations III and IIIa is just 18 ka, compared with 76-118 ka for the last ten “full” glacial-interglacial cycles.

MIS 15b, 13b and 7d are associated with high or rising eccentricity and the associated pronounced high-amplitude fluctuations in precession (Figure 4). The intervals began with major solar troughs followed by equally large upswings in solar radiation through 600-589 kyr and 230-220 kyr in the Northern Hemisphere. At the end of MIS 15b the Northern Hemisphere summer insolation reached one of the highest peaks of the last million years. This pattern of solar radiation changes would have prevented Northern Hemisphere ice-expansion achieving the magnitude reached during full glacial-interglacial cycles. In the case of MIS 15, this pronounced insolation peak would have also impacted on the development of the following glacial-interglacial

cycles encompassing MIS 14, as noted earlier. This highlights how important Northern Hemisphere insolation is in driving glaciations and the structure of glacial-interglacial cycles. Whilst Hughes and Gibbard (2018) found that changes in Northern Hemisphere insolation accounts for c. 50-60% of global glacier changes, the rest is accounted for in regional internal factors. However, that is for 100 kyr glacial-interglacial cycles, and for short “missing” glacial intervals like MIS 15b, 13b and 7d the role of insolation is likely to be even more critical in preventing the development of full glacial-interglacial cycles.

4. Discussion

4.1. “Missing glaciations” – real or apparent?

The hypothesis that global glacier extents were significantly more limited in some glacial-interglacial cycles than others has been tested using a variety of different records. The first and obvious place to look is in the terrestrial record and here notably there is limited evidence of major global glacier extents in MIS 8, 10 and 14. However, this is not to say that there is no evidence of glaciation in intervals such as MIS 8, only that the patterns of global glaciation do not match those of other glacial-interglacial cycles such as MIS 5d-2, 6 and 12. Indeed, in some areas like North-East Asia and Patagonia MIS 8 was characterised by a major glacier advance. A key challenge is understanding the true age of the pre-Illinoian glaciations in North America, for which conclusive evidence remains elusive (Rovey and Balco 2011). Nevertheless, most evidence here and in Europe points to MIS 6 being a larger glaciation than both MIS 10 and 8 in most regions.

The terrestrial record of glaciations can potentially provide a misleading impression of the extent of glaciations during different glacial-interglacial cycles, especially where glacial limits were overridden by later glaciers. Even if this was the case, some “missing glaciations” may have been characterised by ice extents that were similar in size to those in later glaciations. However, MIS 8, 10 and 14 were all characterised by much smaller global sea-level depressions, which supports the idea that these were characterised by glaciers that were relatively limited in extent and volume compared with other glacial-interglacial cycles. Dust records also provide insights into the patterns of ice build-up in these glaciations compared with larger glaciations. In the “missing glaciations”, dust peaks indicate an early global glacier advance that had

more impact on the global hydrological cycle than later in the glacial-interglacial cycle. In the largest glaciations of MIS 5d-2, 6, 12 and 16, the dust peaks were towards the end of glacial-interglacial cycles at the global glacial maxima. The early dust peaks in these big glaciations appear to be associated with glacier advances in high-latitude Asia and globally in the mid-latitude mountains, whereas the later dust peaks correspond with maxima of the large continental ice sheets over North America and Europe (Hughes and Gibbard 2018). In the “missing glaciations” it appears that these early glacier advances had bigger impacts on Antarctic dust flux than the later global glacial maxima. Thus, this analogue suggests that during the “missing glaciations” of MIS 8, 10 and 14 the ice sheets of North America and Europe had much less effect on Antarctic dust flux than in the more extensive glaciations of MIS 5d-2, 6, 12 and 16.

Whilst global glacier extents during MIS 8 and 10 are argued to have been less than in other glacial-interglacial cycles, these intervals are associated with a large ice-rafted debris (IRD) signal in North Atlantic marine sediment sequences (McManus et al. 1999). This is in contrast to the muted signal of the ‘Fleuve Manche’ fluvial discharge through the English Channel during these glaciations (Figure 6). The large IRD signals in MIS 8 and 10 are related to major fluctuations in high-latitude ice-sheet margins around the North Atlantic, whereas the ‘Fleuve Manche’ signal is related to ice-sheet margins further south in the mid-latitudes. Some of these margins are associated with the same ice sheets, such as the British-Irish Ice Sheet. The apparent contradiction of high IRD in the north-eastern Atlantic (McManus et al. 1999), yet limited fluvial discharge associated with ‘Fleuve Manche’ (Toucanne et al. 2009a) suggests a different ice configuration than in later glaciations. Whilst North Atlantic IRD at sites further south and west than ODP 980 is usually dominated by a North American source, background levels of IRD have been linked to the British-Irish Ice Sheet (Bigg et al. 2010). On the continental margin offshore of Ireland, radiogenic isotope source-fingerprinting, in combination with coarse lithic component analysis, indicates a dominant IRD source from the British-Irish ice sheet since the earliest Pleistocene (Thierens et al. 2012). It is therefore possible that the ice sheets over Ireland and Scotland in MIS 8 and 10 were very active, possibly reaching the Atlantic continental shelf as in the last glacial-interglacial cycle (Stoker and Bradwell 2005; Bradwell et al. 2007; Peters et al. 2016), but that this was not matched by

extensive ice further east over England and Wales or continental Europe. Thus, the contrasting evidence for glaciation in MIS 8 and 10 from the high- and mid-latitudes in the NE Atlantic region, as well as across the globe, hints at a major difference in ocean-atmosphere configuration compared with other glacial-interglacial cycles.

The different ocean-atmosphere configurations in MIS 10 and 8 compared with other glaciations in MIS 12, 6 and 5d-2 may be linked to ocean circulation in the North Atlantic and especially North Atlantic deepwater formation. This is known to be affected by the flux of water from the south (Gutjahr et al. 2010) and thus ice sheet-ocean dynamics around Antarctica may have played a significant role in explaining the instability of Northern Hemisphere ice masses in MIS 8 and 10. In fact, as noted earlier, dust flux over Antarctica for MIS 8 was one of the largest and most sustained of the last million years, reaching values comparable with MIS 6 and greater than in MIS 5d-2. This may therefore indicate that global ice volume in MIS 8 was dominated by Southern Hemisphere ice expansion. There is strong evidence of a large glacier advance in Patagonia at *c.* 260 ka. However, elsewhere, in Australasia the evidence for MIS 8 is not so clear, with glaciations MIS 6 and 10 appearing to be larger. Hein et al. (2017, p. 93) wrote that the “cause of the large MIS 8 advance in central Patagonia during a comparatively minor global ice age is unclear, and is an avenue for future research”.

Evidence from the Stocking Glacier in the McMurdo Dry Valleys in Eastern Antarctica shows that the glacier was 20-30% larger than today at 391 ± 35 ka, during MIS 11 (Swanger et al. 2017). It also illustrates that the Dry Valleys have been ice-free for at least the last 350-400 ka. This is important because it suggests that expansion of the East Antarctic Ice Sheet cannot have been a major factor in explaining differences between the last four 100 kyr glacial-interglacial cycles. Instead, it is the smaller and more dynamic West Antarctic Ice Sheet that is most likely to have varied between these glacial-interglacial cycles. West Antarctica is surrounded by the largest area of continental shelf around the continent, with large areas available for ice growth; much larger than around the East Antarctic ice sheet relative to the current size of the respective ice sheets (Figure 7). The West Antarctic Ice Sheet has long been considered to be prone to collapse (Mercer 1984; Pollard and DeConto 2009). The shelf configuration around this region is equally likely to have

777 facilitated rapid and extensive ice build-up during periods of low global sea levels
778 during glaciations. After the Early-Middle-Pleistocene transition it has been suggested
779 that the West Antarctic Ice Sheet shifted to a marine-based configuration (Sutter et al.
780 2019), and it is likely that the nature of this configuration through different
781 subsequent glacial-interglacial cycles would have been a major factor in influencing
782 ice sheet dynamics. However, most glacial geological studies of the West Antarctic
783 Ice Sheet relate to the last glacial-interglacial cycle (e.g. Sugden et al. 2006) with little
784 direct evidence of Middle Pleistocene glacial histories.

785
786 Given the evidence above, any Southern Hemisphere lead associated with Antarctica,
787 must be associated with changes in the West Antarctic Ice Sheet. This is in terms of
788 both ice sheet-atmosphere and ice sheet-ocean interactions, the latter influencing
789 climate in the Northern Hemisphere through both the thermal ocean seesaw (Crowley
790 1992; Stocker and Johnsen 2003; Pedro et al. 2018) and the deep-water seesaw
791 (Broecker 1998). Increased freshwater input from ice sheets as they expanded to the
792 continental shelf causing greater calving loss is likely to have a major impact on
793 Antarctic Meridional Overturning Current which in turn affects the strength of North
794 Atlantic deep-water formation (Swingedouw et al. 2009).

795
796 Thus, extensive West Antarctic Ice Sheets in MIS 8 and 10 may have reduced the
797 strength of the North Atlantic Conveyor, inhibiting moisture delivery to the areas of
798 potential ice-sheet growth in lands bordering the North Atlantic Ocean. In this
799 scenario the early dust peak maxima in both MIS 10 and 8 (Figure 4) would be caused
800 by the Southern Hemisphere lead in ice build-up, which was matched by ice build-up
801 in the Northern Hemisphere, especially over Asia. However, as West Antarctic ice
802 grew larger through the glacial-interglacial cycle this caused a shutdown of the North
803 Atlantic Conveyor starving ice sheets around the North Atlantic Ocean of moisture,
804 explaining their absence from the geological record. This pattern is best suited to
805 explain the nature of glaciations in MIS 8 since the early dust peak is also matched by
806 the lowest global sea levels, which both precede the benthic $\delta^{18}\text{O}$ trough by c. 18 kyr.
807 Whilst MIS 10 exhibited some similarities to MIS 8, it also had similarities with the
808 larger glacier extents of MIS 12, 6 and 5d-2. MIS 14, on the other hand, has strong
809 similarities with MIS 8, especially since both are followed by extended interglacial
810 complexes (MIS 13 and 7, respectively). Hao et al. (2015) argued that MIS 14

inception was a response to changes in Antarctic ice sheets rather than to Northern Hemisphere cooling. However, in MIS 14 it is likely that the West Antarctic Ice Sheet was more restricted and sensitive than in MIS 10 and 8 since there is evidence that the ice sheet collapsed in the interval MIS 15-13 (Hillenbrand et al. 2009). This is possibly due to significantly higher global sea levels during MIS 14 than occurred in other major glaciations (Table 1).

The relatively weak signal of global glaciation within MIS 14 has also been proposed as a direct cause of the extended interglacial complex of MIS 15-13 (Hao et al. 2015). Whilst the strong solar radiation peak that preceded this glaciation in MIS 15a would have mitigated glacier inception in MIS 14, the subsequent weak global glaciation would also have an impact on the extended interglacial that followed (MIS 13). This is also evident in the case of MIS 8, a weak global glaciation which was followed by the extended interglacial complex of MIS 7. This observation also has relevance for subsequent glacial inception, with some cases of failed glacial-interglacial cycles evident in intervals such as MIS 13b and 7d, which succeeded the weak glaciations in MIS 14 and 8, respectively.

4.2. Looking for patterns: the role of orbital forcing in explaining the magnitude of glaciations

There is a clear link between the magnitude of peak-trough variations at the end of interglacials and the intensity of global glaciations in the subsequent cold stage. This is evident in the values of solar-trough magnitude for the last seven glacial-interglacial cycles (Table 2). MIS 8 and 10 are associated with the lowest values of solar-trough magnitude. Lower solar-trough magnitudes at the end of interglacials means that glacier build-up early in the glacier cycles is likely to be less significant than in other glacial-interglacial cycles where solar-trough magnitudes are more pronounced (Table 2). MIS 14 does not follow conform with this theory since it was characterised by a large solar-trough magnitude at the end of MIS 15. However, the preceding solar radiation peak was the largest preceding any of the last seven glacial-interglacial cycles and was associated with maximum eccentricity (Figure 4). In fact, in the last 800 kyr solar radiation only exceeded the MIS 15/14 peak in the Northern Hemisphere summer in the extended interglacial complex of MIS 7 (Figure 4).

As noted earlier, the drivers of global glacial dynamics during the weaker global
glaciations in MIS 8 and 14 appear to have had a southern lead, and to be dominated
by changes in Antarctic ice sheets rather than to Northern Hemisphere cooling. This
suggests that a Northern Hemisphere lead in driving global glaciations through solar
forcing is mitigated by interhemispheric ocean-atmospheric connections (Table 2).
This partly explains why changes in Northern Hemispheric solar radiation can only
explain 50-60% of global ice volume through the last 100 kyr glacial-interglacial
cycles (cf. Hughes and Gibbard 2015). The evidence also suggests that changes in
Northern Hemispheric solar radiation have a much smaller influence in explaining
glacier dynamics during the “missing glaciations”, such as MIS 8 and 14. Whilst there
was a northern lead and quasi-synchronicity in climate for the most severe and largest
glaciations of MIS 16, 12, 6 and 5d-2, driven by changes in solar radiation input to the
Northern Hemisphere (e.g. Mercer 1984), this was not the case for the “missing
glaciations” of MIS 14, 10 and 8. This is important because it shows that solar forcing
was not a significant control on global glaciation during the “missing glaciations”. It
illustrates that the Milankovitch hypothesis cannot explain the structure of all glacial
cycles – a point noticed several decades ago (see references in Mercer 1984). This is
still a significant issue today since the marine isotope record is still tuned to the
pacing of orbital variations (Lisiecki and Raymo 2006) following the findings of Hays
et al. (1976). Whilst this is appropriate for the classic 100 ka glacial cycles such as
MIS 16, 12, 6 and 5d-2 the efficacy of orbital tuning breaks down when dealing with
“missing glaciations” such as MIS 14, 10 and 8. This, and the fact that the marine
oxygen isotope record suffers from spatial bias (i.e. the dominance of the Laurentide
Ice Sheet), means that the established view of glacial-interglacial cycles through the
lens of the marine isotopic curve can be misleading.

There is a potential link between orbital eccentricity and the magnitude of glaciations
over the last five glacial-interglacial cycles. Increasing eccentricity causes increasing
amplitude of variations in the climatological precession parameter ($e \sin \omega$) that
describes how the precession of the equinoxes affects the seasonal configuration of
the Earth-Sun distance (Berger and Loutre, 1991, p. 297). This affects the solar-
trough magnitude at the end of interglacials (Figure 4). Small glaciers can rapidly
build-up in response to mass balance changes associated with a deteriorating climate

(Bahr et al. 1998). This explains why mountain glaciers are often seen to reach their maxima early in glacial-interglacial cycles when precession contrasts are at their greatest (see Hughes et al. 2013; Hughes and Gibbard 2018). However, precessional cycles are too short to sustain larger ice sheet build-up. This means that ice sheets are more likely to sustain build-up during periods of low precessional variability. This was the case in MIS 12 for example (Figure 4). Another important consideration is the effect of diminishing magnitude of precessional cycles through glacial-interglacial cycles, which is displayed during some of the largest glaciations such as in MIS 12 and 5d-2 (Figure 4). In contrast, this effect is much weaker or reversed (i.e. increasing magnitude of precessional cycles) during MIS 8 and 10, respectively. Diminishing precession results in excess ice build-up causing ice sheet instability and collapse during terminations after the fourth or fifth precessional cycles (Raymo 1997; Ridgwell et al. 1999). This is because diminished precession causes smaller changes between the seasons and the negative effects on glacier mass balance of the lengthening of the melt season during upswings to solar peaks is reduced (Hughes and Gibbard 2018).

The sets of consecutive “missing glaciations” in MIS 10 and 8 occurred during a trend towards increasing eccentricity and precession which caused larger amplitude variations in solar radiation, which reached their greatest amplitude in MIS 7 (Figure 4). Other “missing glaciations” in the weak pseudo-glacial-interglacial cycles of MIS 7d, 13b and 15b also correspond with large amplitude solar cycles associated with increased eccentricity and associated precession. This pattern supports the idea that glaciations are influenced by 413 kyr cycles with 100 kyr glacial-interglacial cycles superimposed and modulated by these larger-scale orbital cycles (Rial 1999). However, the relationship is not perfect because MIS 16, one of the major global glaciations, also occurred during a rising trend of eccentricity (Figure 4). However, this earlier eccentricity cycle was less pronounced than that which occurred over the last five glacial-interglacial cycles and the effects on precession were smaller.

4.3. “Missing glaciations” and implications for Quaternary chronostratigraphy

The fact that not all 100 kyr glacial-interglacial cycles produced the same magnitude of ice extent and volume on Earth has major implications for understanding how these

cycles relate to glaciations. This is complicated further when considering shorter term climatic variations and their global glacier imprint. For example, despite being classified within isotope interglacials, MIS 7d and 15b saw global sea-level depressions similar to some glacier maxima within full glacial-interglacial cycles. This highlights the problems of using single proxy records, largely dominated by the marine isotope record, as a measure of the extent and pacing of global glaciations. The fact that marine isotope sequences are tuned by orbital parameters provides a sense of regularity around glacial-interglacial cycles when it is apparent that not all glacial-interglacial cycles are the same, with some very different to others. The lesson from this is that the extent and magnitude of glaciations within glacial-interglacial cycles cannot be deciphered using the marine isotope record alone. This further highlights the problems of correlating terrestrial sequences with the marine isotope record (cf. Gibbard and West 2000) and is a problem not limited to just glacier records (e.g. Bińka and Marks 2018).

For example, for one of the most extensive glaciations of the Quaternary, the Saalian, Wolstonian, Illinoian and equivalents (during MIS 6), both the timing and extent of individual regional glacial advances and retreats vary significantly. In northern Europe, two major stadial advances are recognised during the classical Saalian glaciation, the Late Saalian Drenthe and Warthe Stadial advances, lasting from ~180-160 and 150-140 ka, respectively (Toucanne et al. 2009a; Margari et al. 2014). In the past, these events had been thought to represent separate glaciations, however, there is no evidence of major interstadial or interglacial warming during the intervening interval (Ehlers et al. 2011c). Whilst robust dating now indicates that the two major intervals occurred during the same glaciation, marine records indicate that after ~150 ka ice sheets expanded, with global ice volume reaching the Penultimate Glacial Maximum (PGM) extent towards the end of MIS 6 (i.e. ~140 ka). This principally reflects the growth of the late Illinoian ice sheet in North America (e.g. Curry, et al. 2011; Syverson and Colgan, 2011; Margari et al. 2014). However, in Europe the equivalent Warthe ice advance was markedly less extensive than the Drenthe/Dniepr, although this might have been compensated for by glacial expansion in Russia and Siberia (e.g. Astakhov, 2004). Likewise, the apparent absence of glaciation during MIS 8 (Middle Saalian/pre-Illinoian A) in both western Europe in North America

contrasts with the record in the east, such as in Siberia, where the ice reached its Pleistocene maximum extent at that time.

In recent publications on the Quaternary stratigraphy of northern Germany, and to some extent elsewhere, references to the correlation with marine isotope stages are largely avoided. The number of interglacials between Elsterian and Saalian is still disputed, but the position of the Holsteinian Stage interglacial has gradually moved from MIS 7 (Caspers et al., 1995), via MIS 9 (Litt et al., 2007), to MIS 11 (Ehlers, 2011, Stephan, 2014). If the latter interpretation is correct, except for the Treldenæs Till in Jutland (Denmark), no truly glacial deposits of either MIS 10 or 8 have been identified so far. In the British Isles, the equivalent of the Saalian Stage interval is defined as the Wolstonian in a borehole at Marks Tey in East Anglia. As in Germany (cf. Stephan 2014), the Wolstonian Stage has been plagued by incorrect correlations with the marine isotopic record because of the climatic complexity within it. This is despite Gibbard and Turner (1990) stating that “the Wolstonian Stage includes all time between the end of the Hoxnian [~MIS 11] and the beginning of the Ipswichian [~MIS 5] Stages irrespective of climatic or similar events that may be subsequently identified”. The evidence presented in here shows that whilst there is no doubt that multiple such climatic and glaciation events occurred in MIS 10 and 8, their imprint in the terrestrial sequences is frequently lacking and this highlights why glaciations are time-transgressive events and should not be confused with true chronostratigraphical units in the Quaternary stratigraphical record.

Another consequence of the observations presented here is that for older glaciations, in common with those of the last glacial-interglacial cycle (Weichselian, Wisconsinan, Valdaian, etc.; Hughes et al. 2013; Hughes & Gibbard 2018), it cannot be assumed that ice sheets throughout the world reached their maximum extents at the same time. Rather it appears that asynchronicity is the norm, at least during the major glaciations of the Middle to Late Pleistocene. All these results clearly emphasise the danger of adopting a simplistic counting backward-and-forward approach to extra-regional glacial stratigraphy. Indeed the implications for stratigraphical and modelling reconstructions are profound. The lesson being that simple, one-to-one, uncritical correlations with terrestrial, and in particular with the marine isotope sequences, hold numerous potentially serious pitfalls for the unwary.

5. Conclusions

Glaciations in MIS 8 and 10 were relatively limited in extent in western Europe and North America, in comparison to other Middle Pleistocene glaciations such as the Elsterian/pre-Illinoian B (MIS 12) and the Late Saalian/Illinoian (MIS 6). MIS 14 is notable for being especially marginal as a glacial-interglacial cycle compared with other 100 kyr cycles in terms of glacier extent and related global climatic and environmental indicators. In most areas glaciations were less extensive in MIS 8, 10 and 14 than the Weichselian/Wisconsinan (MIS 5d-2), with a few notable exceptions. For example, east of the Urals in Siberia, the maximum extent of MIS 8 glaciation marks the maximum extent of Pleistocene glaciation in this region. Also, in parts of Patagonia, MIS 8 glaciers were larger than in both MIS 6 and 5d-2.

The records for MIS 8 and 10 differ from other glacial-interglacial cycles in that there is evidence for pronounced dust peaks in Antarctic ice cores early on with smaller dust peaks towards the end of the glacial-interglacial cycles during global glacier maxima. The early dust peak in the last glacial-interglacial cycle (MIS 5d-2) is associated with early advances of glaciers in the mid-latitude mountains, continental interiors, and especially Arctic Asia and in mountains bordering the NW Pacific Ocean (Batchelor et al. 2019). By analogy, this implies that MIS 8 and 10 saw large glaciations in these regions but less significant continental ice sheet expansions around the North Atlantic margins. This is supported by sea-level evidence, with global sea-level depressions 20-30 m less in MIS 8 and 10 compared to that during MIS 12, 6 and 2. However, early dust peaks in MIS 8 are also closely related to significant ice expansion in Patagonia suggesting a Southern-Hemisphere lead. The relationship between Southern and Northern Hemisphere glaciations is likely to be affected by the dynamics of the West Antarctic Ice Sheet and the effects of its expansion on ocean circulation through oceanic bipolar seesaws.

Solar forcing plays a major role in determining the size and length of glaciations. Over the long term, the “missing glaciations” of the last five glacial-interglacial cycles are associated with rising eccentricity and increased precession. Whilst this accelerates glacier build-up in the short term during pronounced insolation downturns, it hinders their build-up during the following upswing. For example, the amplitude of

solar precession associated with peak eccentricity can be linked to failed glacial-interglacial cycles such as MIS 7d and 15b. These short intense stadials were prevented from developing into full glacial-interglacial cycles directly because of the pattern of Northern Hemisphere solar variations.

The fact that 100 kyr glacial-interglacial cycles produced glaciations of very different magnitudes in different places around the globe poses problems when relying on a global indicator of glacier change, as is often the case when using the marine isotopic record. This has important implications for using the marine isotope record as a basis for understanding glaciations on land and wider terrestrial records. The structure of glacial-interglacial cycles, whilst predictable when considering the largest glaciations, is much less clear when considering weaker global glaciations in MIS 8, 10 and 14. The spatial and temporal patterns of glaciation were different in these glacial-interglacial cycles compared to the strongest glaciations of the last 500 kyr in MIS 12, 6 and 5d-2. This indicates that glacial-interglacial cycles are not as predictable as is suggested in marine isotopic records that are tuned by orbital cycles.

Acknowledgements

We thank Editor Nicholas Lancaster, Associate Editor Pat Bartlein and two anonymous reviewers for detailed and very helpful comments on an initial draft of this paper. We also thank Graham Bowden and Nick Scarle for drawing the figures.

References

- Arndt, J.E., H. W. Schenke, M. Jakobsson, F. Nitsche, G. Buys, B. Goleby, M. Rebesco, F. Bohoyo, J.K. Hong, J. Black, R. Greku, G. Udintsev, F. Barrios, W. Reynoso-Peralta, T. Morishita, R. Wigley, "The International Bathymetric Chart of the Southern Ocean (IBCSO) Version 1.0 - A new bathymetric compilation covering circum-Antarctic waters", 2013, *Geophysical Research Letters*, Vol. 40, p. 3111-3117, [doi: 10.1002/grl.50413](https://doi.org/10.1002/grl.50413)
- Astakhov, V., 2004. Pleistocene ice limits in Russian northern lowlands. In: Ehlers, J., Gibbard, P.L. (Eds.), *Quaternary Glaciations - Extent and Chronology. Part 1: Europe*. Elsevier, Amsterdam, p. 309-319.

1047

1048 Astakhov, V., 2011. Ice margins of northern Russia revisited. In: Ehlers, J., Gibbard,

1049 P.L., Hughes, P.D., (Eds). In: Ehlers, J., Gibbard, P.L. and Hughes, P.D. (Eds)

1050 Quaternary Glaciations - Extent and Chronology, Part IV - A Closer Look.

1051 Amsterdam: Elsevier. p. 1-14.

1052

1053 Astakhov, V., Shkatova, V., Zastrozhnov, A., Chuyko, M., 2016.

1054 Glaciomorphological map of the Russian Federation. Quaternary International 420, 4-

1055 14.

1056

1057 Bahr, D.B., Pfeffer, W.T., Sassolas, C., Meier, M.F., 1998. Response time of glaciers

1058 as a function of size and mass balance:1. Theory. Journal of Geophysical Research

1059 103, 9777-9782.

1060

1061 Barendregt and Duk-Rodkin 2011. Chronology and Extent of Late Cenozoic Ice

1062 Sheets in North America: A Magnetostratigraphical Assessment. In: Ehlers, J.,

1063 Gibbard, P.L., Hughes, P.D. (Eds.), Quaternary Glaciations - Extent and Chronology:

1064 A Closer Look. Developments in Quaternary Science, 15. Elsevier, Amsterdam, pp.

1065 419-426.

1066

1067 Barrell, D.J.A., 2011. Quaternary Glaciers of New Zealand. In: Ehlers, J., Gibbard,

1068 P.L., Hughes, P.D. (Eds.), *Quaternary Glaciations – Extent and Chronology – A*

1069 *Closer Look*. Developments in Quaternary Sciences, Elsevier, vol. 15, pp. 1047–1064.

1070

1071 Barrows, T.T., Stone, J.O., Fifield, L.K., Cresswell, R.G., 2002. The timing of the last

1072 glacial maximum in Australia. Quaternary Science Reviews 21, 159-173.

1073

1074 Batchelor, C.L., Margold, M., Krapp, M., Murton, D.K., Dalton, A.S., Gibbard, P.L.,

1075 Stokes, C.R., Murton, J.B., Manica, A., 2019. The configuration of Northern

1076 Hemisphere ice sheets through the Quaternary. Nature Communications 10:3713.

1077 <https://doi.org/10.1038/s41467-019-11601-2>.

1078

1079 Beets, D., Meijer, T., Beets, C., Cleveringa, P., Laban, C., van der Spek, A., 2005.
 1080 Evidence for a middle Pleistocene glaciation of MIS 8 age in the southern North Sea.
 1081 Quaternary International 133–134, 7–19.
 1082

1083 Berger, A., 1992, Orbital Variations and Insolation Database. IGBP PAGES/World
 1084 Data Center for Paleoclimatology Data Contribution Series # 92-007. NOAA/NGDC
 1085 Paleoclimatology Program, Boulder CO, USA.
 1086

1087 Berger, A., Loutre, M.F., 1991. Insolation values for the climate of the last 10 million
 1088 years. Quaternary Sciences Reviews 10, 297-317.
 1089

1090 Bigg, G.R., Levine, R.C., Clark, C.D., Greenwood, S.L., Haflidason, H., Hughes,
 1091 A.L.C., Nygård, A., Sejrup, H.P., 2010. Last glacial ice-rafted debris off southwest
 1092 Europe: the role of the British-Irish Ice Sheet. Journal of Quaternary Science 25, 689-
 1093 699.
 1094

1095 Biňka, K., Marks, L., 2018. Terrestrial versus marine archives: biostratigraphical
 1096 correlation of the Middle Pleistocene lacustrine records from central Europe and their
 1097 equivalents in the deep-sea cores from the Portuguese margin. Geological Quarterly
 1098 62, 69-80. doi: 10.7306/gq.1395
 1099

1100 Bintanja, R., Roderik, S.W., van de Wal, O.J., 2005. Modeled atmospheric
 1101 temperatures and global sea levels over the past million years, Nature, 437, 125-128.
 1102

1103 Bolliger, T., Feijfar, O., Graf, H.R. & Kalin, D.W. 1996. Vorläufige Mitteilung über
 1104 Funde von pliozanen Kleinsäugern aus den Höheren Deckenschottern des Juras (Kt.
 1105 Zürich). Eclogae geologicae Helvetiae 89, 1043–1048.
 1106

1107 Bolshiyakov, D.Y., Savatuygin, L.M., Shneider, G.V., Molodkov, A.N., 1998. New
 1108 data about modern and ancient glaciations of the Taimyr-Severozemlskaya region.
 1109 Materialnyy glyachologicheskikh issledovaniy 85, 219-222 (in Russian).
 1110

1111 Bradwell, T., Stoker, M., Larter, R. 2007. Geomorphological signature and flow
 1112 dynamics of the Minch palaeo-ice stream, NW Scotland. *Journal of Quaternary*
 1113 *Science* 22, 609–617.
 1114

1115 Braun, D. 2011. The glaciation of Pennsylvania, USA. In: Ehlers, J., Gibbard, P.L.,
 1116 Hughes, P.D. (Eds.), *Quaternary Glaciations - Extent and Chronology: A Closer*
 1117 *Look*. *Developments in Quaternary Science*, 15. Elsevier, Amsterdam, pp. 521–530.
 1118

1119 Bridgland, D.R., Howard, A.J., White, M.J., White, T.S. (eds) (2014): *Quaternary of*
 1120 *the Trent*. Oxbow Books, Oxford, 416 pp.
 1121

1122 Broecker, W.S., 1998. Paleocean circulation during the last deglaciation: a bipolar
 1123 seesaw? *Paleoceanography* 13, 119-121.
 1124

1125 Broecker, W.S., van Donk, J., 1970. Insolation changes, ice volumes, and the O¹⁸
 1126 record in deep-sea cores. *Reviews of Geophysics* 8, 169–198.
 1127

1128 Calvet, M., 2004. The Quaternary glaciations of the Pyrenees. In: Ehlers, J. and
 1129 Gibbard, P. L. (editors): *Quaternary Glaciations – Extent and Chronology. Part I,*
 1130 *Europe*. *Developments in Quaternary Science* 2, 119–128. Amsterdam, Elsevier.
 1131

1132 Caspers, G., Jordan, H., Merkt, J., Meyer, K.-D., Müller, H, Streif, H., 1995.
 1133 Niedersachsen. In: Benda, L. (Ed.), *Das Quartär Deutschlands*, Stuttgart,
 1134 Borntraeger, 23-58.
 1135

1136 Cheng, H., Edwards, L., Broecker, W.S., Denton, G.H., Kong, X., Wang, Y., Zhang,
 1137 R., Wang, X., 2009. Ice Age Terminations. *Science* 326, 248-252, doi:
 1138 10.1126/science.1177840
 1139

1140 Claquin, T., Roelandt, C., Kohfeld, K., Harrison, S., Tegen, I., Prentice, I.,
 1141 Balkanski, Y., Bergametti, G., Hansson, M., Mahowald, N., Rodhe, H., Schulz, M.,
 1142 2003. Radiative forcing of climate by ice-age atmospheric dust. *Climate Dynamics*
 1143 20, 193-202.

1144 Clark, P.U., Pollard, D., 1998. Origin of the Middle Pleistocene Transition by ice
1145 sheet erosion of regolith. *Paleoceanography* **13**, 1–9.

1146

1147 Cohen, K.M., Gibbard, P., 2011. Global chronostratigraphical correlation table for the
1148 last 2.7 million years. Subcommission on Quaternary Stratigraphy (International
1149 Commission on Stratigraphy), Cambridge, England.

1150 <http://quaternary.stratigraphy.org/charts/>

1151

1152 Colhoun, E.A., 1985. The Glaciations of the West Coast Range, Tasmania.
1153 *Quaternary Research* 24, 39-59.

1154

1155 Colhoun, E.A., Barrows, T.T., 2011. The glaciation of Australia. In: Ehlers, J.,
1156 Gibbard, P.L., Hughes, P.D. (Eds.), *Quaternary Glaciations – Extent and Chronology*
1157 *– A Closer Look*. Developments in Quaternary Sciences, Elsevier, vol. 15, pp. 1037–
1158 1045.

1159

1160 Crowley, T., 1992. North Atlantic deepwater cools the Southern Hemisphere.
1161 *Paleoceanography* 7, 489-497.

1162

1163 Curry, B.B., Grimley, D.A. & McKay, E.D. III, 2011, Quaternary glaciations in
1164 Illinois, in Ehlers, J., Gibbard, P.L. & Hughes, P.D., eds, *Quaternary Glaciations -*
1165 *Extent and Chronology - A Closer Look: Developments in Quaternary Science* 15, p.
1166 467-487.

1167

1168 Davies, B.J., Roberts, D.H., Bridgland, D.R., Ó Cofaigh, C., Riding, J.B., Demarchi,
1169 B., Penkman, K., Pawley, S.M., 2012. Timing and depositional environments of a
1170 Middle Pleistocene glaciation of northeast England: New evidence from Warren
1171 House Gill, County Durham. *Quaternary Science Reviews* 44, 180-212.

1172

1173 Demuro, M., Froese, D., Arnold, L., Roberts, R. 2012. Single-grain OSL dating of
1174 glaciofluvial quartz constrains Reid glaciation in NW Canada to MIS 6. *Quaternary*
1175 *Research*, 77(2), 305-316.

1176

1177 Doppler, G., Kroemer, E., Rögner, K., Wallner, J., Jerz, H. & Grottenthaler, W. 2011.

1178 Quaternary Stratigraphy of Southern Bavaria. *E & G Quaternary Science Journal*

1179 60(2-3), 329-365.

1180

1181 Duk-Rodkin, A., Barendregt, R.W., Froese, D.G., Weber, F., Enkin, R.J., Smith, I.R.,

1182 Zazula, G.D., Waters, P., Kalssen, R., 2004. Timing and extent of Plio-Pleistocene

1183 glaciations in North-Western Canada and East-Central Alaska. In: Ehlers, J., Gibbard,

1184 P.L. (Eds.), *Quaternary Glaciations—Extent and Chronology. Part II: North America*.

1185 Elsevier, Amsterdam, pp. 313–345.

1186

1187 Duk-Rodkin, A., Barendregt, R.W., 2011. Stratigraphical record of

1188 glacials/interglacials in Northwest Canada. In: Ehlers, J., Gibbard, P.L., Hughes, P.D.

1189 (Eds.), *Quaternary Glaciations – Extent and Chronology – A Closer Look*.

1190 *Developments in Quaternary Sciences*, Elsevier, vol. 15, pp. 661–698.

1191

1192 Dyke, A.S., Prest, V.K., 1987. Late Wisconsinan and Holocene History of the

1193 Laurentide Ice Sheet". *Géographie Physique et Quaternaire*. 41, 237-263.

1194

1195 Ehlers, J., 2011. *Das Eiszeitalter*. Spektrum, Heidelberg. 372 pp.

1196

1197 Ehlers, J., Gibbard, P.L., Hughes, P.D. (Eds) 2011a. *Quaternary Glaciations - Extent*

1198 *and Chronology, Part IV - A Closer Look*. Amsterdam: Elsevier. 1108 pp.

1199

1200 Ehlers, J., Gibbard, P.L., Hughes, P.D. 2011b. Quaternary Glaciations - Extent and

1201 Chronology, Part IV - a closer look: Introduction. In: Ehlers, J., Gibbard, P.L. and

1202 Hughes, P.D. (Eds) *Quaternary Glaciations - Extent and Chronology, Part IV - A*

1203 *Closer Look*. Amsterdam: Elsevier. p. 1-14.

1204

1205 Ehlers, J., Grube, A., S. H-J., Wansa, S., 2011c. Pleistocene glaciations of North

1206 Germany – New Results. In: Ehlers, J., Gibbard, P.L. and Hughes, P.D. (Eds.),

1207 *Quaternary Glaciations – Extent and Chronology: A Closer Look*. *Developments in*

1208 *Quaternary Science*, 16. Elsevier: Amsterdam. p. 149-162.

1209

1210 Ehlers, J., Gibbard, P.L., Hughes, P.D., 2018. Quaternary glaciations and chronology.
 1211 In: Menzies, J., van der Meer, J.J.M., (Eds). Past Glacial Environments. Elsevier. 2nd
 1212 Edition. p. 77-101.
 1213
 1214 Elderfield, H., Ferretti, P., Greaves, M., Crowhurst, S., McCave, N., Hodell, D.,
 1215 Piotrowski, A.M., 2012. Evolution of Ocean Temperature and Ice Volume Through the
 1216 Mid-Pleistocene Climate Transition. *Science* 337, 704-709.
 1217
 1218 Evans, D.J.A., Roberts, D.H., Bateman, M.D., Ely, J., Medialdea, A., Burke, M.J.,
 1219 Chiverrell, R.C., Clark, C.D., Fabel, D., 2019. A chronology for North Sea Lobe
 1220 advance and recession on the Lincolnshire and Norfolk coasts during MIS 2 and 6.
 1221 *Proceedings of the Geologists' Association*.
 1222 <https://doi.org/10.1016/j.pgeola.2018.10.004>
 1223
 1224 Fernández Mosquera, D., Marti, K., Vidal Romaní, J.R., Weigel, D., 2000. Late
 1225 Pleistocene deglaciation chronology in the NW of the Iberian Peninsula using cosmic-
 1226 ray produced ²¹Ne in quartz. *Nuclear Instruments and Methods in Physical Research*
 1227 B 172, 832–837
 1228
 1229 Fiebig, M., Ellwanger, D., Doppler, G., 2011. Pleistocene Glaciations of Southern
 1230 Germany. In: Ehlers, J., Gibbard, P.L. and Hughes, P.D. (Eds) Quaternary Glaciations
 1231 - Extent and Chronology, Part IV - A Closer Look. Amsterdam: Elsevier. p. 163-174.
 1232
 1233 Fitzsimons, S.J., Colhoun, E.A., van de Geer, G., 1990. Middle Pleistocene glacial
 1234 stratigraphy at Baxter Rivulet, western Tasmania, Australia. *Journal of Quaternary*
 1235 *Science* 5, 17-27.
 1236
 1237 Fitzsimons, S.J., Colhoun, E.A., van de Geer, G., Pollington, M., 1992. The Quaternary
 1238 geology and glaciation of the King Valley. *Geological Survey Bulletin* 68, 1-57
 1239 Tasmanian Department of Mines, Hobart.
 1240
 1241 Fletcher, W.J., Müller, U.C., Koutsodendris, A., Christanis, K., Pross, J. 2013. A
 1242 centennial-scale record of vegetation and climate variability from 312 to 240ka

1243 (Marine Isotope Stages 9c-a, 8 and 7e) from Tenaghi Philippon, NE Greece.
 1244 Quaternary Science Reviews 78, 108-125.
 1245
 1246 Fullerton, D.S., Colton, R.B., Bush, C.A., 2004. Limits of mountain and continental
 1247 glaciations east of the Continental Divide in northern Montana and north-western
 1248 North Dakota, U.S.A. In: Ehlers, J., Gibbard, P.L. (Eds.), Quaternary Glaciations -
 1249 Extent and Chronology. Part 2: North America. Elsevier, Amsterdam, p. 131-150.
 1250
 1251 Ganopolski, A., Winkelmann, R., Schellnhuber, H.J., 2016. Critical insolation–CO₂
 1252 relation for diagnosing past and future glacial inception. Nature 529, 200-203.
 1253
 1254 Ganopolski, A., Calov, R., 2011. The role of orbital forcing, carbon dioxide and
 1255 regolith in 100 kyr glacial cycles. Climate of the Past 7, 1415–1425.
 1256
 1257 Gibbard, P.L., Turner, C., 1990. Cold stage type sections: some thoughts on a difficult
 1258 problem. Quaternaire 1, 33-40.
 1259
 1260 Gibbard, P.L., West, R.G. 2000. Quaternary chronostratigraphy: the nomenclature of
 1261 terrestrial sequences. Boreas 29, 329-336.
 1262
 1263 Gibbard, P.L., Clark, C.D., 2011. Pleistocene Glaciation Limits in Great Britain. In:
 1264 Ehlers, J., Gibbard, P.L. and Hughes, P.D. (Eds) Quaternary Glaciations - Extent and
 1265 Chronology, Part IV - A Closer Look. Amsterdam: Elsevier. p. 75-94.
 1266
 1267 Gibbard, P.L., West, R.G., Hughes, P.D., 2018. Pleistocene glaciation of Fenland,
 1268 England, and its implications for evolution of the region. Royal Society Open Science
 1269 4, 170736. <http://dx.doi.org/10.1098/rsos.170736>.
 1270
 1271 Gillespie, A., Molnar, P., 1995. Asynchronous maximum advances of mountain and
 1272 continental glaciers. Reviews of Geophysics 33, 311-364.
 1273
 1274 Gillespie, A.R., Zehfuss, P.H., 2004. Glaciations of the Sierra Nevada, California,
 1275 USA. In: Ehlers, J., Gibbard, P.L. (Eds.), Quaternary Glaciations - Extent and
 1276 Chronology. Part 2: North America. Elsevier, Amsterdam, p. 131-150.

1277

1278 Gillespie, A.R., Clark, D.H., 2011. Glaciations of the Sierra Nevada, California, USA.

1279 In: Ehlers, J., Gibbard, P.L. and Hughes, P.D. (Eds) *Quaternary Glaciations - Extent*

1280 *and Chronology, Part IV - A Closer Look*. Amsterdam: Elsevier. p. 447-462.

1281

1282 Giraudi, C. and Giaccio, B., 2017. Middle Pleistocene glaciations in the Apennines,

1283 Italy: new chronological data and preservation of the glacial record. Geological

1284 Society, London, Special Publications, 433, 161-178.

1285

1286 Giraudi, C., Bodrato, G., Ricci Lucchi, M., Cipriani, N., Villa, I.M., Giaccio, B.,

1287 Zuppi, G.M., 2011. The Middle and late Pleistocene glaciations in the Campo Felice

1288 basin (Central Apennines, Italy). *Quaternary Research* 75, 219-230.

1289

1290 Graham, A.G.C., 2007. Reconstructing Pleistocene Glacial Environments in the

1291 Central North Sea Using 3D Seismic and Borehole Data. Ph.D. thesis, University of

1292 London, 410 pp.

1293

1294 Graham, A.G.C., Stoker, M.S., Lonergan, L., Bradwell, T., Stewart, M.A., 2011. The

1295 Pleistocene glaciations of the North Sea Basin. In: Ehlers, J., Gibbard, P.L., Hughes,

1296 P.D. (Eds.), *Quaternary Glaciations – Extent and Chronology – A Closer Look*.

1297 *Developments in Quaternary Sciences*, Elsevier, vol. 15, pp. 261–278.

1298

1299 Gutjahr, M., Hoogakker, B.A.A., Frank, M., McCave, N., 2010. Changes in North

1300 Atlantic Deep Water strength and bottom water masses during Marine Isotope Stage 3

1301 (45-35 ka BP). *Quaternary Science Reviews* 29, 2451-2461.

1302

1303 Hao, Q., Wang, L., Oldfield, F., Guo, Z., 2015. Extra-long interglacial during MIS

1304 15-13 arising from limited extent of Arctic ice sheets in glacial MIS 14. *Scientific*

1305 *Reports* 5, 12103. DOI: 10.1038/srep12103

1306

1307 Hays, J.D., Imbrie, J., Shackleton, N.J., 1976. Variations in the Earth's orbit:

1308 pacemaker of the ice ages. *Science* 194, 1121-1132.

1309

1310 Head, M.J., Gibbard, P.L., 2005. Early-Middle Pleistocene transitions: an overview
 1311 and recommendations for the defining boundary. Geological Society, London, Special
 1312 Publications 247, 1-18.
 1313

1314 Head, M.J., Gibbard, P.L., 2015. Formal subdivision of the Quaternary
 1315 System/Period: past, present, and future. Quaternary International 383, 4-35.
 1316

1317 Head, M.J., Pillans, B., Farquhar, S.R., 2008. The Early–Middle Pleistocene
 1318 Transition: characterization and proposed guide for the defining boundary. Episodes
 1319 31, 255-259.
 1320

1321 Hein, A.S., Hulton, N.R.J., Dunai, T.J., Schnabel, C., Kaplan, M.R., Naylor, M., Xu,
 1322 S., 2009. Middle Pleistocene glaciation in Patagonia dated by cosmogenic-nuclide
 1323 measurements on outwash gravels. Earth and Planetary Science Letters 286, 184-197.
 1324

1325 Hein, A.S., Coge, A., Darvill, C.M., Mendelova, M., Kaplan, M.R., Herman, F.,
 1326 Dunai, T.J., Norton, K., Xu, S., Christl, M., Rodés, Á. 2017. Regional mid-
 1327 Pleistocene glaciation in central Patagonia. Quaternary Science Reviews 164, 77-94.
 1328

1329 Hillenbrand, C.-D., Kuhn, G., Frederichs, T., 2009. Record of a Mid-Pleistocene
 1330 depositional anomaly in West Antarctic continental sediments: an indicator for ice-
 1331 sheet collapse. Quaternary Science Reviews 28, 1147-1159.
 1332

1333 Hobbs, W.W., 1945. The Greenland Glacial Anticyclone. Journal of Meteorology 2,
 1334 143-153.
 1335

1336 Houmark-Nielsen, M., 2004. The Pleistocene of Denmark: a review of stratigraphy and
 1337 glaciation history. In: Ehlers, J., Gibbard, P.L. (Eds.), Quaternary Glaciations—
 1338 Extent and Chronology. Part I, Europe. Elsevier, Amsterdam, pp. 35–46.
 1339

1340 Houmark-Nielsen, M., 2011. Pleistocene glaciations in Denmark: A closer look at
 1341 chronology, ice dynamics and landforms. In: Ehlers, J., Gibbard, P.L., Hughes, P.D.
 1342 (Eds.), *Quaternary Glaciations – Extent and Chronology – A Closer Look*.
 1343 Developments in Quaternary Sciences, Elsevier, vol. 15, pp. 47–58.

1344

1345 Hughes, P.D., Gibbard, P.L., 2018. Global glacier dynamics during 100 ka

1346 Pleistocene glacial cycles. *Quaternary Research* 90, 222-243.

1347

1348 Hughes, P.D., Woodward, J.C., van Calsteren, P.C., Thomas, L.E. 2011. The Glacial

1349 History of The Dinaric Alps, Montenegro. *Quaternary Science Reviews* 30, 3393-

1350 3412.

1351

1352 Hughes, P.D., Gibbard, P.L., Ehlers, J. 2013. Timing of glaciation during the last

1353 glacial cycle: evaluating the meaning and significance of the ‘Last Glacial Maximum’

1354 (LGM). *Earth Science Reviews* 125, 171-198.

1355

1356 Imbrie, J., Hays, J.D., Martinson, D.G., McIntyre, A., Mix, A.C., Morley, J.J., Pisias,

1357 N.G., Prell, W.L., Shackleton, N.J., 1984. The orbital theory of Pleistocene climate:

1358 support from a revised chronology of the marine ^{18}O record. In: Berger, A., Imbrie, J.,

1359 Hays, G., Kukla, G., Saltzman, B. (Eds.), *Milankovitch and Climate*. Reidel,

1360 Dordrecht, pp. 269–306.

1361

1362 Kiernan, K., Fink, D., Greig, D., Mifud, C., 2010. Cosmogenic radionuclide

1363 chronology of pre-last glacial cycle moraines in the Western Arthur Range, Southwest

1364 Tasmania. *Quaternary Science Reviews* 29, 3286-3297.

1365

1366 Kukla, G., An, Z. S., Melice, J. L., Gavin, J., Xiao, J. L., 1994. Magnetic

1367 susceptibility record of Chinese Loess. *Transactions of the Royal Society of*

1368 *Edinburgh, Earth Science*, **81**, 263–288.

1369

1370 Lambert, F., Delmonte, B., Petit, J.R., Bigler, M., Kaufmann, P.R., Hutterli, M.A.,

1371 Stockler, T.F., Ruth, U., Steffensen, J.P., Maggi, V., 2008. Dust–climate couplings

1372 over the past 800,000 years from the EPICA Dome C ice core. *Nature* 452, 616-619.

1373

1374 Lambert, F., Bigler, M., Steffensen, J.P., Hutterli, M., Fischer, H., 2012. Centennial

1375 mineral dust variability in high-resolution ice core data from Dome C, Antarctica.

1376 *Climate of the Past* 8, 609-623.

1377

1378 Lang, N., Wolff, E.W., 2011. Interglacial and glacial variability from the last 800 ka
 1379 in marine, ice and terrestrial archives. *Climate of the Past* 7, 361-380. doi:10.5194/cp-
 1380 7-361-2011
 1381
 1382 Lewis, A.N., 1945. Pleistocene glaciation in Tasmania. *Papers and Proceedings - The*
 1383 *Royal Society of Tasmania* 1944, 41-56.
 1384
 1385 Lindner, L., Marks, L., 1999. New approach to stratigraphy of palaeolake and glacial
 1386 sediments of the younger Middle Pleistocene in mid-eastern Poland. *Geological*
 1387 *Quarterly* 43 (1), 1-8.
 1388
 1389 Lisiecki, L.E., Raymo, M.E., 2005. A Pliocene-Pleistocene stack of 57 globally
 1390 distributed benthic $\delta^{18}\text{O}$ records. *Paleoceanography* 20, PA1003,
 1391 doi:10.1029/2004PA001071
 1392
 1393 Litt, T., Behre, K.-E., Meyer, K.-D., Stephan, H.-J., and Wansa, S., 2007.
 1394 *Stratigraphische Begriffe für das Quartär des norddeutschen Vereisungsgebietes,*
 1395 *E&G Quaternary Science Journal* 56, 7-55
 1396
 1397 Manabe, S., Broccoli, A.J. 1985. The influence of continental ice sheets on the
 1398 climate of an ice age. *Journal of Geophysical Research* 90, D1, 2167-2190.
 1399
 1400 Margari, V., Skinner, L.C., Tzedakis, P.C., Ganopolski, A., Vautravers, M.,
 1401 Shackleton, N.J., 2010. The nature of millenniascale climate variability during the
 1402 past two glacial periods. *Nature Geoscience* 3, 127-131.
 1403
 1404 Margari, V., Skinner, L.C., Hodell, D.A., Martrat, B., Toucanne, S., Grimalt, J.O.,
 1405 Gibbard, P.L., Lunkka, J.P., Tzedakis, P.C., 2014. Land-ocean changes on orbital and
 1406 millennial time scales and the penultimate glaciation. *Geology* 42, 183-186.
 1407
 1408 Marks, L., 2011. Quaternary glaciations in Poland. In: Ehlers, J., Gibbard, P.L. and
 1409 Hughes, P.D. (Eds.), *Quaternary Glaciations – Extent and Chronology: A Closer*
 1410 *Look. Developments in Quaternary Science*, 15. Elsevier: Amsterdam, pp. 299-304.
 1411

1412 McManus, J.F., Oppo, D.W., Cullen, J.L., 1999. A 0.5 million-year record of
 1413 millennial-scale climate variability in the North Atlantic. *Science*, 283, 971-975.
 1414
 1415 Mercer, J.H., 1984. Simultaneous climatic change in both hemispheres and similar
 1416 bipolar interglacial warming: evidence and implications. In: Hansen, J.E., Takahashi,
 1417 T., *Climate Processes and Climate Sensitivity*. Geophysical Monograph Series 29,
 1418 307-313.
 1419
 1420 Mudelsee, M., Schulz, M., 1997. The Mid-Pleistocene transition: onset of 100 ka
 1421 cycle lags ice volume build-up by 280 ka. *Earth and Planetary Science Letters* 151,
 1422 117-123.
 1423
 1424 Muttoni, G., Carcano, C., Garzanti, E., Ghielmi, M., Piccin, A., Pini, R., et al., 2003.
 1425 Onset of Pleistocene glaciations in the Alps. *Geology* 31, 989-992.
 1426
 1427 Ottesen, D., Dowdeswell, J.A. & Bugge, T. 2014. Morphology, sedimentary infill and
 1428 depositional environments of the Early Quaternary North Sea Basin (56-62 Grad N).
 1429 *Marine and Petroleum Geology* 56, 123-146.
 1430
 1431 Pedro, J.B., Jochum, M., Buizert, C., He, F., Barker, S., Rasmussen, S.O., 2018.
 1432 Beyond the bipolar seesaw: Towards a process understanding of interhemispheric
 1433 cooling. *Quaternary Science Reviews* 192, 27-46.
 1434
 1435 Peters, J.L., Benetti, S., Dunlop, P., Ó Cofaigh, C., Moreton, S.G., Wheeler, A.J.,
 1436 Clark, C.D., 2016. Sedimentology and chronology of the advance and retreat of the
 1437 last British-Irish Ice Sheet on the continental shelf west of Ireland. *Quaternary*
 1438 *Science Reviews* 140. 101-124.
 1439
 1440 Pollard, D., DeConto, R.M., 2009. Modelling West Antarctic ice sheet growth and
 1441 collapse through the past five million years. *Nature* 458, 329-333.
 1442
 1443 Preusser, F., Graf, H.R., Keller, O., Krayss, E., Schlüchter, C., 2011. Quaternary
 1444 glaciation history of northern Switzerland. *E&G Quaternary Science Journal* 60, 282-
 1445 305.

1446

1447 Railsback, L.B., Gibbard, P.L., Head, M.J., Voarintsoa, N.R.G., Toucanne, S., 2015.

1448 An optimized scheme of lettered marine isotope substages for the last 1.0 million

1449 years, and the climatostratigraphic nature of isotope stages and substages. *Quaternary*

1450 *Science Reviews* 111, 94-106.

1451

1452 Rattenbury, M.S., Townsend, D.B., Johnston, M.R., (compilers), 2006. *Geology of*

1453 *the Kaikoura area. Institute of Geological & Nuclear Sciences 1:250,000 Geological*

1454 *Map 13. GNS Science, Lower Hutt, New Zealand.*

1455

1456 Rial, J.A., 1999. Pacemaking the ice ages by frequency modulation of Earth's orbital

1457 eccentricity. *Science* 285, 5427, 564-568.

1458

1459 Richmond, G.M., 1986. Stratigraphy and correlation of glacial deposits of the Rocky

1460 Mountains, the Colorado Plateau & the ranges of the Great Basin. *Quaternary Science*

1461 *Reviews* 5, 99-127.

1462

1463 Richmond, G.M., Fullerton, D.S., 1986. Summation of Quaternary glaciations in the

1464 United States of America. In: Sibrava, V., Bowen, D.Q., Richmond, G.M. (Eds.)

1465 *Quaternary Glaciations in the Northern Hemisphere, Quaternary Science Reviews* 5,

1466 183-196.

1467

1468 Rohling, E. J., Grant, K., Bolshaw, M., Roberts, A. P., Siddall, M., Hemleben, C., and

1469 Kucera, M. 2009. Antarctic temperature and global sea level closely coupled over the

1470 past five glacial cycles. *Nature Geoscience* 2, 500-504.

1471

1472 Rohling, E. J., Grant, K. M., Bolshaw, M., Roberts, A. P., Siddall, M., Hemleben, C.,

1473 Kucera, M., Foster, G. L., Marino, G., Roberts, A. P., Tamisiea, M. E., and Williams,

1474 F., 2014. Sea-level and deep-sea-temperature variability over the past 5.3 million

1475 years. *Nature* 508, 477-482.

1476

1477 Roskosch, J. Winsemann, J., Polom, U., Brandes, C., Tsukamoto, S., Weitkamp, A.,

1478 Bartholomäus, W.A., Henningsen, D., Frechen, M., 2015. Luminescence dating of

1479 ice-marginal deposits in northern Germany: evidence for repeated glaciations during
1480 the Middle Pleistocene (MIS 12 to MIS 6). *Boreas*, 44, 103-126.

1481

1482 Rother, H., Shulmeister, J., Rieser, U., 2010. Stratigraphy, optical dating chronology
1483 (IRSL) and depositional model of pre-LGM glacial deposits in the Hope Valley, New
1484 Zealand. *Quaternary Science Reviews* 29, 576-592.

1485

1486 Roucoux, K.H., Tzedakis, P.C., Frogley, M.R., Lawson, I.T., Preece, R.C., 2008.
1487 Vegetation history of the Marine Isotope Stage 7 interglacial complex at Ioannina,
1488 NW Greece. *Quaternary Science Reviews* 27, 1378-1395.

1489

1490 Roucoux, K.H., Tzedakis, P.C., de Abreu, L., Shackleton, N.J., 2006. Climate and
1491 vegetation changes 180,000 to 345,000 years ago recorded in a deep-sea core off
1492 Portugal. *Earth and Planetary Science Letters* 249, 307-325.

1493

1494 Rovey, C.W., Balco, G., 2011. Summary of early and middle Pleistocene glaciations
1495 in northern Missouri, USA. In: Ehlers, J., Gibbard, P.L., Hughes, P.D. (Eds.),
1496 *Quaternary Glaciations – Extent and Chronology – A Closer Look*. Developments in
1497 Quaternary Sciences, Elsevier, vol. 15, pp. 553-561.

1498

1499 Ruddiman, W.F., McIntyre, A., 1982. Severity and speed of Northern Hemisphere
1500 glaciation pulses: The limiting case? *Geological Society of America Bulletin* 93,
1501 1273-1279.

1502

1503 Ruddiman, W.F., Raymo, M.E., Martinson, D.G., Clement, B.M., Backman, J., 1989.
1504 Pleistocene evolution of Northern Hemisphere climate. *Paleoceanography* 4, 353-412.

1505

1506 Rudenko, T.A., Fainer, Yu.B., Fainer, T.G., 1984. National Geological Map of the
1507 USSR, Scale 1:1 000 000, New Series, Quadrangle P48,49 (Vanavara). Map of
1508 Quaternary Deposits. VSEGEI, Leningrad.

1509

1510 Ruth, U., Bigler, M., Rothlisberger, R., Siggaard-Andersen, M.L., Kipfstuhl, S., Goto-
1511 Azuma, K., Hansson, M.E., Johnsen, S.J., Lu, H.Y., Steffensen, J.P., 2007. Ice core

1512 evidence for a very tight link between North Atlantic and east Asian glacial climate.
 1513 Geophysical Research Letters 34 (3), L03706. doi:10.1029/2006GL027876.
 1514
 1515 Schlüchter, C. 1989. A non-classical summary of the Quaternary stratigraphy in the
 1516 northern Alpine Foreland of Switzerland. Bulletin de la Société neuchâteloise de
 1517 géographie 32 – 33, 143-157.
 1518
 1519 Scourse, J.D., Austin, W.E.N., Sejrup, H.P., Ansair, M.H., 1999. Foraminiferal
 1520 isoleucine epimerization 353 determinations from the Nar Valley Clay, Norfolk, UK:
 1521 implications for Quaternary correlations in the 354 southern North Sea basin.
 1522 Geological Magazine 136, 543-560.
 1523
 1524 Sejrup, H.P., Larsen, E., Landvik, J., King, E.L., Haflidason, H., Nesje, A., 2000.
 1525 Quaternary glaciations in southern Fennoscandia: evidence from southwestern
 1526 Norway and the northern North Sea region. Quaternary Science Reviews 19, 667-685.
 1527
 1528 Sejrup, H.P., Hjelstuen, B.O., Dahlgren, K.I.T., Haflidason, H., Kuijpers, A., Nygård,
 1529 A., Praeg, D., Stoker, M., Vorren, T.O., 2005. Pleistocene glacial history of the NW
 1530 European continental margin. Marine and Petroleum Geology 22, 1111-1129.
 1531
 1532 Shackleton, N.J., 1967. Oxygen isotope Analyses and Pleistocene Temperatures Re-
 1533 assessed. Nature 215, 15-17.
 1534
 1535 Shakun, J. D., Lea, D.W., Lisiecki, L.E., Raymo, M.E., 2015. An 800-kyr record of
 1536 global surface ocean $\delta^{18}\text{O}$ and implications for ice volume-temperature coupling.
 1537 Earth and Planetary Science Letters 426, 58-68.
 1538
 1539 Singer, B., Ackert, R.P., Guillou, H., 2004. $^{40}\text{Ar}/^{39}\text{Ar}$ and K-Ar chronology of
 1540 Pleistocene glaciations in Patagonia. Geological Society of America Bulletin 116,
 1541 434-450.
 1542
 1543 Sosdian, S. and Rosenthal, Y., 2009. Deep-Sea Temperature and Ice Volume Changes
 1544 Across the Pliocene-Pleistocene Climate Transitions, Science, 325, 306-310.
 1545

1546 Spooner, I.S., Osborn, D.G., Barendregt, R.W., Irving, E., 1996. A Middle
 1547 Pleistocene (Isotope stage 10) glacial sequence in the Stikine River valley, British
 1548 Columbia. *Canadian Journal of Earth Sciences* 33, 1428-1438.
 1549
 1550 Spratt, R.M., Lisiecki, L.E., 2016. A Late Pleistocene sealevel stack. *Climate of the*
 1551 *Past* 12, 1079-1092. doi:10.5194/cp-12-1079-2016
 1552
 1553 Stoker, M.S., Bradwell, T. 2005. The Minch palaeo-ice stream, NW sector of the
 1554 British-Irish ice sheet. *Journal of the Geological Society, London* 162, 425–428.
 1555
 1556 Stiff, B.J., Hansel, A.K., 2004. Quaternary glaciations in Illinois. In: Ehlers, J.,
 1557 Gibbard, P.L. (Eds.), *Quaternary Glaciations—Extent and Chronology*, vol. II, North
 1558 America. Elsevier, Amsterdam, pp. 71–82.
 1559
 1560 Stokes, C., Tarasov, L., Dyke, A.S., 2012. Dynamics of the north American Ice Sheet
 1561 Complex during its inception and build-up to the Last Glacial Maximum. *Quaternary*
 1562 *Science Reviews* 50, 86-104.
 1563
 1564 Stocker, T.F., Johnsen, S.J., 2003. A minimum thermodynamic model for the bipolar
 1565 seesaw. *Paleoceanography* 18, 4, 1087, doi:10.1029/2003PA00092
 1566
 1567 Stephan, H-J., 2014. Climato-stratigraphic subdivision of the Pleistocene in
 1568 Schleswig-Holstein, Germany and adjoining areas. *E&G Quaternary Science Journal*
 1569 63, 3-18.
 1570
 1571 Sugden, D.E., Bentley, M.J., Ó Cofaigh, C., 2006. Geological and geomorphological
 1572 insights into Antarctic ice sheet evolution. *Philosophical Transactions of the Royal*
 1573 *Society A* 364, 1607-1625.
 1574
 1575 Sutter, J., Fischer, H., Grosfeld, K., Karlsson, N.B., Kleiner, T., Van Liefferinge, B.,
 1576 Eisen, O., 2019. Modelling the Antarctic Ice Sheet across the mid-Pleistocene
 1577 transition – implications for Oldest Ice. *The Cryosphere* 13, 2023-2041.
 1578

1579 Svendsen J.I., Alexanderson, H., Astakhov, V.I., Demidov, I., Dowdeswell, J.A.,
 1580 Funder, S., Gataullin, V., Henriksen, M., Hjort, C., Houmark-Nielsen, M., Hubberten,
 1581 H.-W., Ingólfsson, Ó., Jakobsson, M., Kjær, K.H., Larsen, E., Lokrantz, H., Pekka, J.,
 1582 Lunkka Lyså, A., Mangerud, J., Matiouchkov, A., Murray, A., Möller, P., Niessen, F.,
 1583 Nikolskaya, O., Polyak, L., Saarnisto, M., Siegert, C., Siegert, M.J., Spielhagen, R.F.,
 1584 Stein, R., 2004. Late Quaternary ice sheet history of northern Eurasia. *Quaternary*
 1585 *Science Reviews* 23, 1229-1271.
 1586
 1587
 1588 Swanger, K.M., Lamp, J.L., Winckler, G., Schaefer, J.M., Marchant, D.R., 2017.
 1589 Glacier advance during Marine Isotope Stage 11 in the McMurdo Dry Valleys of
 1590 Antarctica. *Scientific Reports* 7, 41433.
 1591
 1592 Swingedouw, D., Fichefet, T., Goosse, H., Loutre, M.F., 2009. Impact of transient
 1593 freshwater releases in the Southern Ocean in the AMOC and climate. *Climate*
 1594 *Dynamics* 33, 365-381.
 1595
 1596 Syverson, K.M., Colgan, P.M., 2004. The Quaternary of Wisconsin: a review of
 1597 stratigraphy and glaciation history. In: Ehlers, J., Gibbard, P.L. (Eds.), *Quaternary*
 1598 *Glaciations—Extent and Chronology. Part II: North America*. Elsevier, Amsterdam,
 1599 pp. 295–311.
 1600
 1601 Syverson, K.M., Colgan, P.M., 2011. The Quaternary of Wisconsin: An Updated
 1602 Review of Stratigraphy, Glacial History and Landforms. In: Ehlers, J., Gibbard, P.L.,
 1603 Hughes, P.D. (Eds.), *Quaternary Glaciations – Extent and Chronology: A Closer*
 1604 *Look. Developments in Quaternary Science* 15. Elsevier, Amsterdam, p. 537-552.
 1605
 1606 Tabor, C.R., Poulsen, C.J., 2016. Simulating the mid-Pleistocene transition through
 1607 regolith removal. *Earth and Planetary Science Letters* 434, 231-240.
 1608

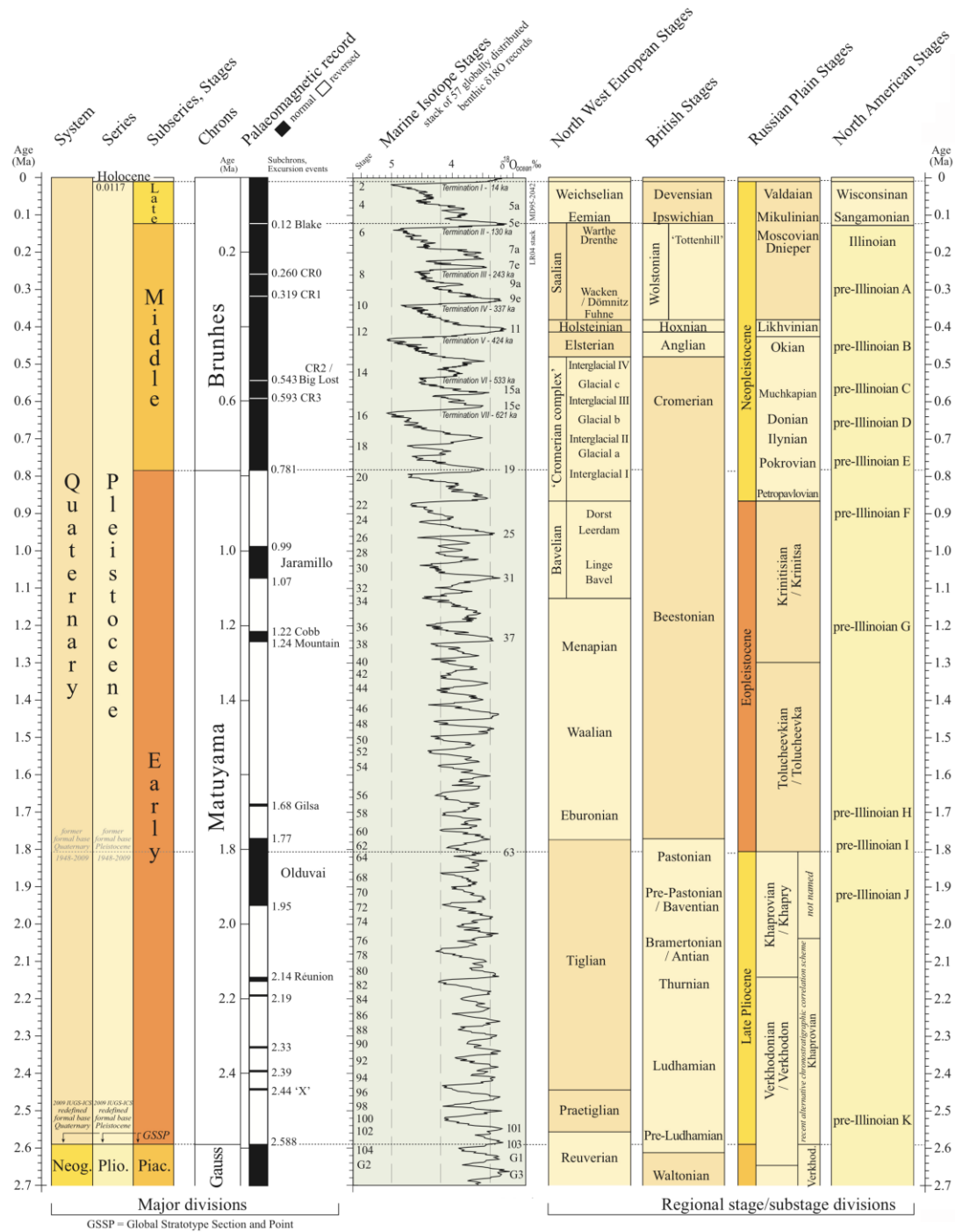
1609 Thierens, M., Pirlet, H., Colin, C., Latruwe, K., Vanhaecke, F., Lee, J.R., Stuut J.-B.,
 1610 Titschack, J., Huvenne, V.A.I., Dorschel, B., Wheeler, A.J., Henriët, J.-P. 2012. Ice-
 1611 rafting from the British-Irish ice sheet since the earliest Pleistocene (2.6 million years
 1612 ago): implications for long-term mid-latitudinal ice-sheet growth in the North Atlantic
 1613 region. *Quaternary Science Reviews* 44, 229-240.
 1614
 1615 Toucanne, S., Zaragosi, S., Bourillet, J.F., Cremer, M., Eynaud, F., Van Vliet-Lanoe,
 1616 B., Penaud, A., Fontanier, C., Turon, J.L., Cortijo, E., Gibbard, P.L., 2009a. Timing of
 1617 massive 'Fleuve Manche' discharges over the last 350 kyr: insights into the European
 1618 ice-sheet oscillations and the European drainage network from MIS 10 to 2.
 1619 *Quaternary Science Reviews* 28, 1238-1256.
 1620
 1621 Toucanne, S., Zaragosi, S., Gibbard, P.L., Bourillet, J.F., Cremer, M., Eynaud, F.,
 1622 Giraudeau, J., Turon, J.L., Cremer, M., Cortijo, E., Martinez, P., Rossignol, L.,
 1623 2009b. A 1.2 my record of glaciation and fluvial discharge from the West European
 1624 continental margin. *Quaternary Science Reviews* 28, 2974-2981.
 1625
 1626 Van Husen, D., Reitner, J.M. 2011. An Outline of the Quaternary Stratigraphy of
 1627 Austria. *E & G Quaternary Science Journal* 60(2-3), 366-387.
 1628
 1629 Velichko, A.A., Faustova, M.A., Pisareva, V.V., Gribchenko, Y.N., Sudakova, N.G.,
 1630 Lavrentiev, N.V., 2011. Glaciations of the East European Plain—distribution and
 1631 chronology. In: Ehlers, J., Gibbard, P.L., Hughes, P.D. (Eds.), *Quaternary*
 1632 *Glaciations – Extent and Chronology – A Closer Look*. Developments in Quaternary
 1633 Sciences, Elsevier, vol. 15, pp. 337-360.
 1634
 1635 Vidal Romani, Fernández, Mosquera, D., Marti, K., 2015. The glaciation of Serra de
 1636 Quiexa-Invernadoiro and Serra do Gerês, NW Iberia. A critical review and a
 1637 cosmogenic nuclide (^{10}Be and ^{21}Ne) chronology. *Cadernos Laboratorio Xeolóxico de*
 1638 *Laxe*, 38, 27-45.
 1639
 1640 Waelbroeck, C., Labeyrie, L., Michel, E., Duplessy, J.C., McManus, J.F., Lambeck,
 1641 K., Balbon, E., Labracherie, M., 2002. Sea-level and deep water temperature changes
 1642 derived from benthic foraminifera isotopic records. *Quaternary Science Reviews* 21,

1643 295-305.
 1644
 1645
 1646 Ward, B.C., Bond, J.D., Froese, D., Jensen, B., 2008. Old Crow tephra (14010 ka)
 1647 constrains penultimate Reid glaciation in central Yukon Territory. *Quaternary Science*
 1648 *Reviews* 27, 1909-1915.
 1649
 1650 White, T.S., Bridgland, D.R., Howard, A.J., Westaway, R., White, M.J., 2010.
 1651 Evidence from the Trent terrace archive, Lincolnshire, UK, for lowland glaciation of
 1652 Britain during the Middle and Late Pleistocene. *Proceedings of the Geologists'*
 1653 *Association* 121, 141-153.
 1654
 1655 White, T.S., Bridgland, D.R., Westaway, R., Straw, A., 2017. Evidence for a late
 1656 Middle Pleistocene glaciation of the British margin of the southern North Sea. *Journal*
 1657 *of Quaternary Science* 32, 261-275.
 1658
 1659 Willeit, M., Ganopolski, A., Calov, R., Brovkin, V., 2019. Mid-Pleistocene transition
 1660 in glacial cycles explained by declining CO₂ and regolith removal. *Science Advances*
 1661 5, eaav7337. 8 pp.
 1662

1663 **Figures**

1664

1665 **Figure 1.** Global correlations between terrestrial glacial chronostratigraphical terms
1666 and the marine oxygen isotope record. Adapted from the global chronostratigraphical
1667 correlation table for the past 2.7 million years by Cohen and Gibbard (2011).



1668

1669

Figure 2. Maximum extent of glaciation around the globe during the last glacial-interglacial cycle (Weichselian, Wisconsinan, Valdaian Stage and equivalents). The extents depicted here are diachronous with ice masses reaching their maximum positions at different times. The extents would have also varied in different glacial-interglacial cycles, although the general differences in extents of the largest continental ice masses is typical of the relative contributions of ice on Earth by the major regional ice masses. This figure illustrates the relative sizes of the ice masses and their spatial distributions and highlights the spatial dominance of the ice masses in the Northern Hemisphere. Redrawn and adapted from Ehlers and Gibbard (2007) and Hughes et al. (2013).

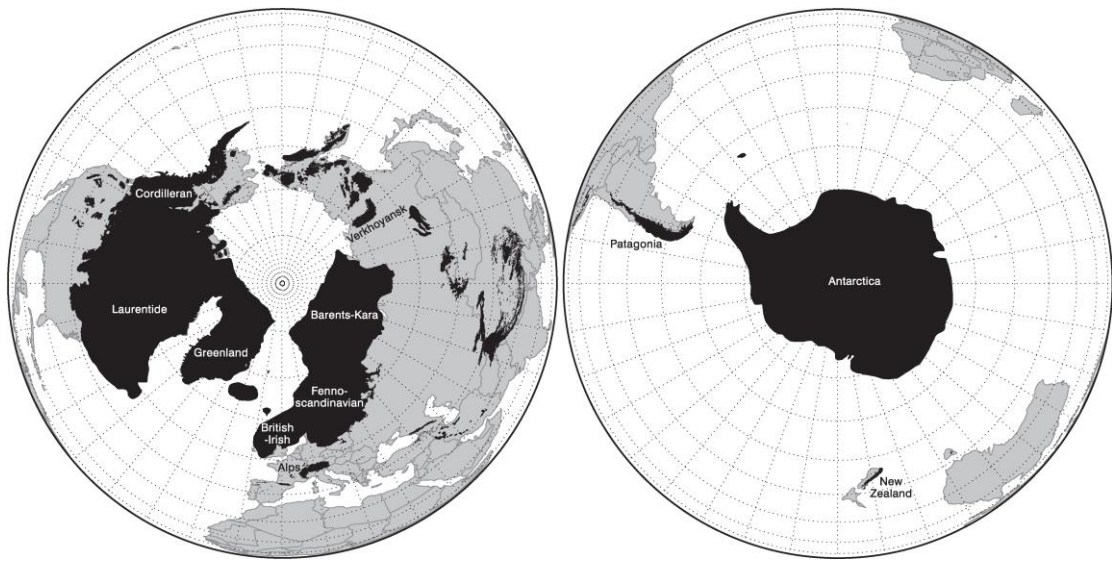


Figure 3. The dust records from Greenland (NGRIP) and Antarctica (EPICA) ice cores for the last glaciation in MIS 5d-2. The top diagram shows the dust concentration (Ruth et al., 2007) record from the NGRIP core (on the GICC05 age model). The bottom diagram shows dust flux (Lambert et al., 2012) from EPICA, Antarctica (on the EDC3 age model). The records show a strong correlation in dust records between Greenland and Antarctica and this supports the assertion that dust records in either polar hemisphere reflect the state of the global hydrological cycle and the global atmosphere. This observation provides the template for interpreting earlier glaciations with drier and dustier atmosphere directly related to increasing global ice coverage. This interhemispheric comparability is important because beyond the last interglacial reliance has currently to be made on the Antarctic ice-core records.

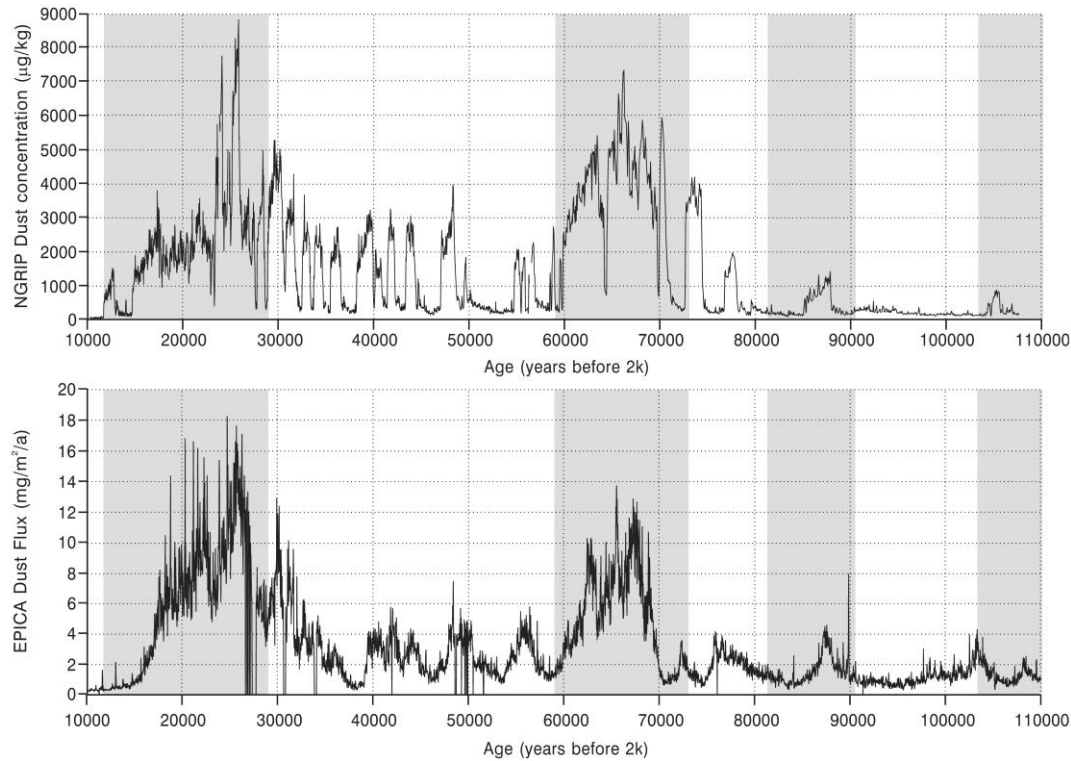
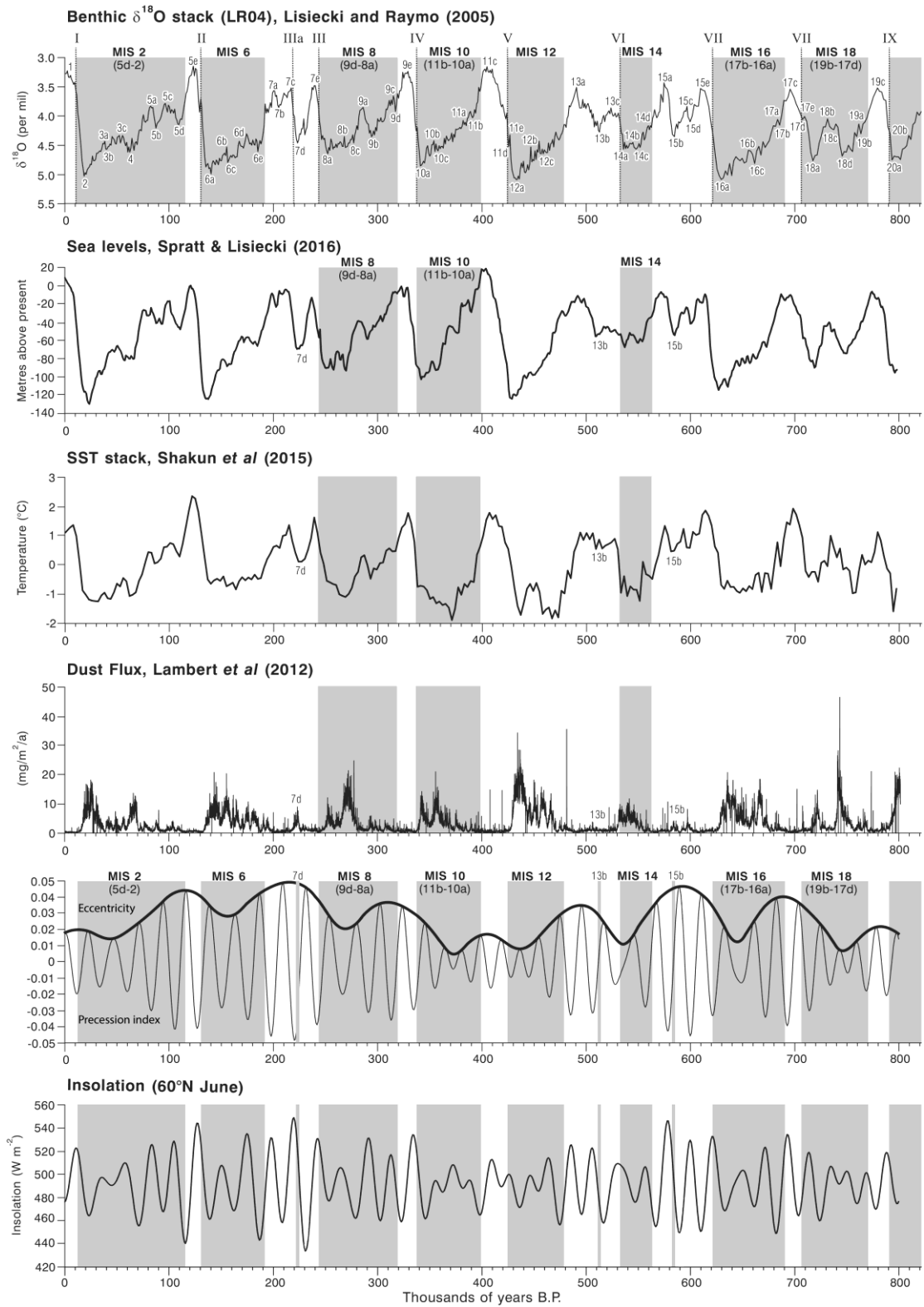


Figure 4. Graphs showing link between the structure of glacial-interglacial cycles indicated in the global benthic stack of Lisiecki and Raymo (2005), global sea levels extracted from a global of seven sea-level records (from Spratt and Lisiecki 2016), global sea-surface temperatures from a 49 paired sea-surface temperature-planktonic $\delta^{18}\text{O}$ records (Shakun et al. 2015) and dust flux from the EPICA Dome C ice-core record (Lambert et al. 2012). The Roman numerals (I, II, III, IV etc.) over the global benthic stack indicate the positions of the respective glacial terminations. The lower two graphs illustrate solar parameters for the last 800 ka. The second from bottom graph shows the precession index and the eccentricity index from Berger and Loutre (1991) and Berger (1992). The precession index (climatological precession parameter: $e \sin \omega$; values from -1 to +1) is an indicator of the amplitude of the seasonal cycle with a move towards autumn/winter perihelion at peaks and towards an earlier spring/summer perihelion at troughs and is determined by the variations in eccentricity (dimensionless value between 0 and 1). The bottom graph shows June insolation data at 60°N (Berger and Loutre 1991; Berger 1992).

See next page



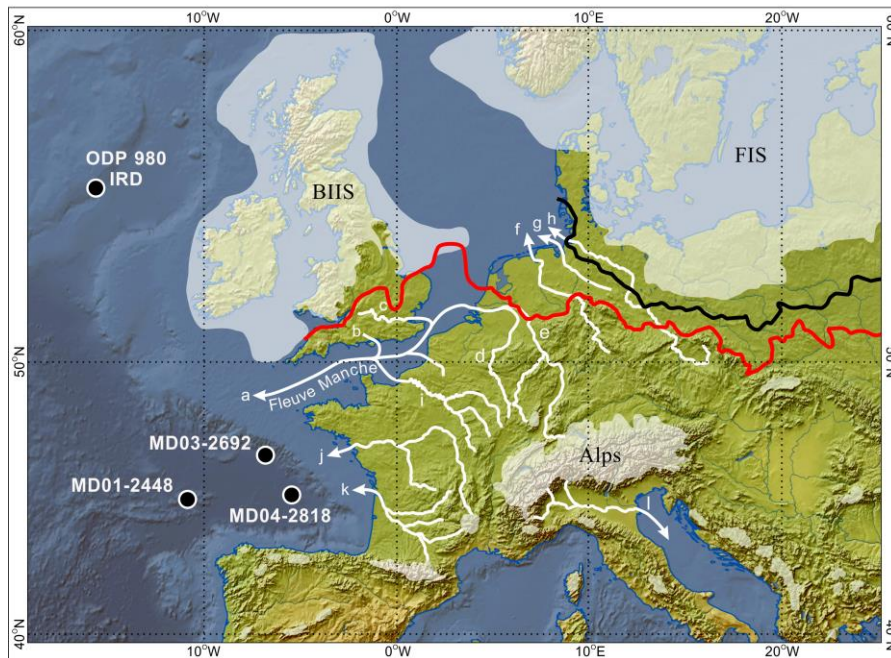
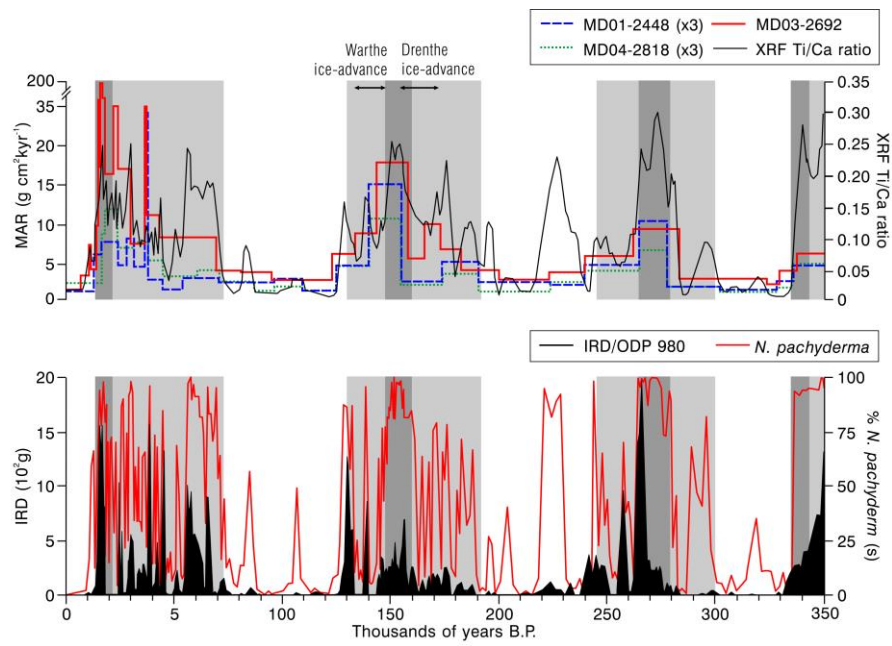
1716
1717
1718

Figure 5. Limits of the Eurasian contiguous ice sheets during the Middle and Late Pleistocene. Adapted from information in Svendsen et al. (2004), Ehlers and Gibbard (2004), and Astakhov et al. (2016). East of the Urals, the most extensive glaciation occurred in MIS 8, although evidence of this glaciation is largely absent to the west in Europe.



Figure 6. Top diagram: mass accumulation rates (MAR) in marine sediment records in the Bay of Biscay, NE Atlantic Ocean (from Toucanne et al. 2009a). The MAR graph is from sites MD03-2692 (46°49.720'N, 9°30.970'W), MD01-2448 and MD04-2818. Lower mass accumulation rates (MAR) in MIS 10 and 8 compared with MIS 5d-2 and 6 are interpreted as indicating less glaciofluvial discharge, primarily through the former English Channel fluvial system (Fleuve Manche). The XRF Ti-Ca ratio reflects terrigenous sediment input, but is also associated with an ice-rafted debris source. The ice-rafted debris (IRD) graph is from site ODP 980 from further north in the NE Atlantic Ocean (55°29'N, 14°42'W) off the British-Irish continental shelf (data from McManus et al. 1999). The bottom map shows the locations of these core sites relative to the former ice masses. The approximate positions of the Late Pleistocene ice limits for the northern ice sheets (BIIS = British-Irish Ice Sheet; FIS= Fennoscandian Ice Sheet) are given for reference in white shading together with the Late Saalian (MIS 6) ice limits shown in red/grey [Drenthe advance] and black [Warthe advance]. The outlines and positions of ice masses in central and southern Europe are schematic due to scale. The white arrows and the associated lowercase letters identify the main European rivers: a: 'Fleuve Manche', b: Solent, c: Thames, d: Meuse, e: Rhine, f: Ems, g: Wesser, h: Elbe, i: Seine, j: Loire, k: Gironde, l: Pô. Redrawn and adapted from Toucanne et al. (2009a).

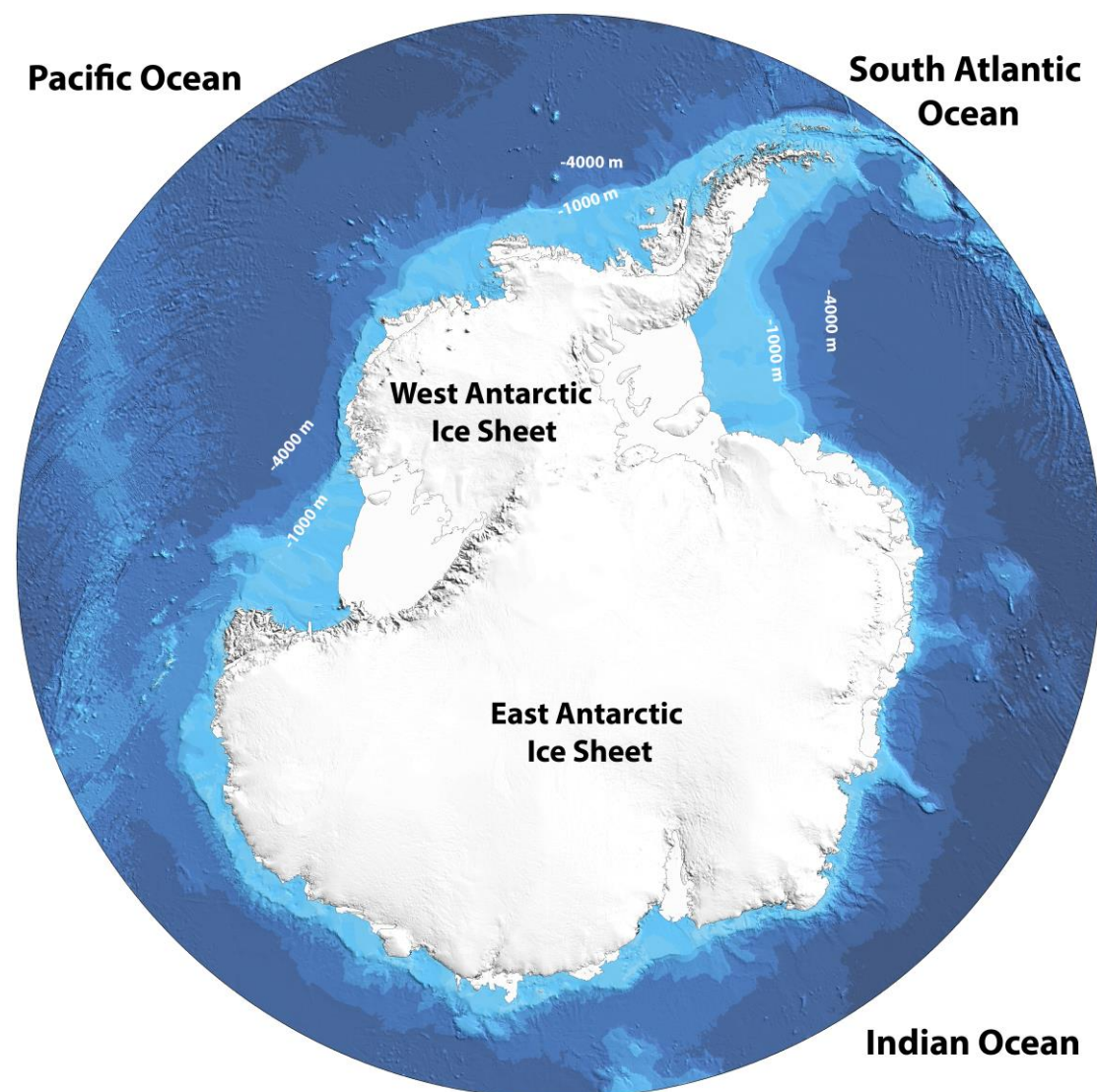
See next page



1747

1748

Figure 7. Topographic map of Antarctica showing offshore bathymetry. The largest area of the currently unglaciated continental shelf is off West Antarctica. This means that there was likely to have been greater scope for ice-sheet expansion to the shelf edge during Pleistocene glaciations than around the East Antarctic Ice Sheet. Thus, the West Antarctic Ice Sheet would have been the most significant ice mass in the Southern Hemisphere in terms of changing dynamics through glacial-interglacial cycles. From the International Bathymetric Chart of the Southern Ocean (IBCSO) Version 1.0 (Arndt et al. 2018). <https://www.scar.org/science/ibcsa/resources/>



Tables

Table 1. Sea-level estimates from the global stack of Spratt and Lisiecki (2016) in order of magnitude. These values are obtained from the long stack (0-798 ka) of five sea level reconstructions. The marine isotope stages listed represent cold-climate intervals within glacial-interglacial cycles. *MIS 15b, 13b and 7d are stadials within interglacials (cf. Hughes et al. 2018).

	MIS	Global sea-level minima (m) – in descending order of magnitude
	2	-130
	6	-124.5
	12	-124.4
	16	-114.62
“Missing glaciations”	10	-102.83
	8	-93.27
	7d*	-68.74
	14	-67.39
	13b*	-55.45
	15b*	-54.40

1772 **Table 2.** Solar radiation peak-trough amplitude at 60°N early in cold stages or at the end of preceding interglacials. Solar-trough magnitude
 1773 describes the peak-trough magnitude and timespan. This is derived by taking the median value between the preceding solar peak and subsequent
 1774 trough and scaling (dividing) this by the peak to trough timespan, then inverting this calculated value. Solar radiation data are derived from
 1775 Berger and Loutre (1991) and Berger (1992).

	Marine Isotope Stage	preceding peak*	age (ka)	trough*	age (ka)	amplitude change	median peak-trough*	peak-trough timespan (kyr)	solar-trough magnitude
	MIS 7/6	531.96	198	443.00	187	88.96	487.48	11	0.0226
	MIS 13/12	525.83	486	456.22	475	69.61	491.03	11	0.0224
	MIS 17/16	534.77	693	448.99	682	85.78	491.88	11	0.0224
	MIS 5e/5d-2	544.69	127	440.20	116	104.49	492.45	11	0.0223
“Missing glaciations”	MIS 9/8	517.25	313	459.83	303	57.42	488.54	10	0.0205
	MIS 11/10	508.45	373	484.84	363	23.61	496.65	10	0.0201
	MIS 15/14	546.62	579	454.66	567	91.96	500.64	12	0.0240

1776
 1777 * insolation (W m⁻²)
 1778